Nuclear molecules

Rep. Prog. Phys. **60** (1997) 819–861. Printed in the UK PII: S0034-4885(97)07907-4

Nuclear molecules

R R Betts†‡ and A H Wuosmaa†

† Physics Division, Argonne National Laboratory Argonne, IL 60439, USA
‡ Physics Department, University of Illinois at Chicago Chicago, IL 60607, USA

Received 12 March 1997

Abstract

We review the subject of nuclear molecular states as exemplified by the experimental observations of narrow resonances in the scattering and reactions of heavy ions. These states are at high excitation energy and sometimes high angular momentum and have very large partial decay widths into symmetric and near symmetric partitions. The experimental data accumulated over the past 30 years are summarized and various theoretical models discussed.

0034-4885/97/080819+43$59.50

Contents

1. Introduction

The term 'nuclear molecule' evokes a picture of a nuclear system having a density distribution with two or more well defined centres similar to well known atomic molecules as schematically shown in figure 1. In the atomic case these centres are naturally provided by the positions of the positively-charged atomic nuclei which produce the Coulomb potential in which the electrons move. The properties of atomic molecules, binding, excitation spectra etc, are then largely defined by the geometric symmetries of the nuclear positions which determine the energies and degeneracies of the electronic orbits in the corresponding multi-centre Coulomb potential. In the nuclear case, there are no such well defined centres and the potential in which the nucleons move arises from the sum of interactions between any one nucleon and all the others. It is, therefore, not at all obvious that molecule-like configurations of nuclei should display any degree of stability. As we shall describe, however, there is now abundant evidence that nuclear molecules do indeed exist and their understanding has shed much new light on aspects of nuclear collective motion and the dynamics of nuclear collisions at low energies.

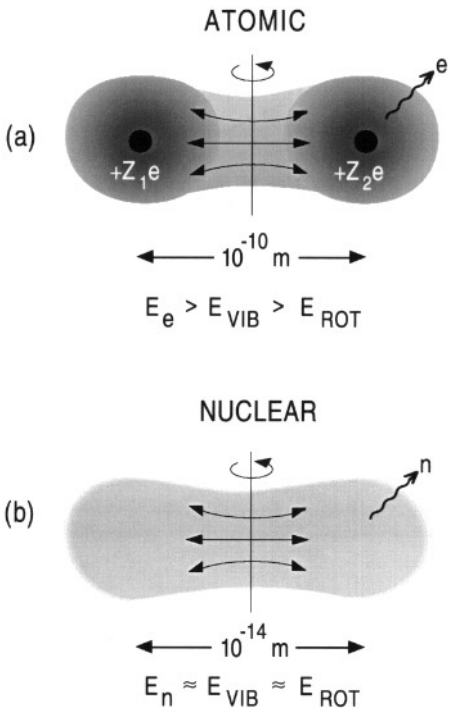

Figure 1. Conceptual comparison of (a) atomic and (b) nuclear molecules.

Although the above geometric picture of molecule-like nuclear configuration is intuitively appealing, the shape of a nuclear system is not, in general, directly observable (although moments of the charge and matter distributions may be). It is, therefore, usual to define the structure of a nuclear configuration in terms of the overlap of the wavefunction with particular partitions of the system a so-called 'spectroscopic factor' or 'reduced width'. In the case of a resonance, this is defined as the ratio of the observed decay width into a

specific channel to the 'single-particle' or Wigner limit given by

$$\Gamma_{\rm sp} = \frac{3\hbar^2}{2\mu R^2} 2P_l(kR)$$

where μ is the reduced mass of the decay channel, R the radius of the confining potential, and $P_l(kR)$ the Coulomb penetrability appropriate to the energy of the decay. Nuclear molecular configurations are defined as states which have unusually large spectroscopic factors for partitions involving the symmetric (or more complex) splitting of the system, for example $^{24}\mathrm{Mg} \rightarrow {}^{12}\mathrm{C} + {}^{12}\mathrm{C}$.

The excitation spectra of atomic molecules arise from three separate degrees of freedom: (a) excitation of the electrons, (b) vibrations in the coordinate describing the separation of the atomic nuclei and (c) rotations of the molecule as a whole about its various symmetry axes. As, in general, $E_{\rm e} > E_{\rm vib} > E_{\rm rot}$ these degrees of freedom are largely uncoupled. In the nuclear case, this is quite different. Both the single-nucleon excitation and rotational energies for even modest angular momentum are comparable. Even though the energies associated with vibrations along the internuclear coordinate are not, *a priori*, known, our knowledge of collective nuclear motion leads us to suspect that the energy associated with this degree of freedom will also be of the same scale. We, therefore, expect that the excitation spectra of nuclear molecules will be more complex than the atomic case, reflecting much stronger coupling between the intrinsic, vibrational and rotational degrees of freedom.

Historically, it was recognized quite early on that certain states in light nuclei possessed very large reduced widths for decay by alpha particle emission. In particular, the ground state of ^{8}Be decays by alpha emission with a width corresponding to a wavefunction with almost complete overlap with a dumbbell-shape configuration of two alpha particles. This notion is underlined by the existence in ^{8}Be of a rotational sequence of states, $J^{\pi} = 0^{+}, 2^{+}, 4^{+}$ observed as resonances in α–α elastic scattering, with a moment of inertia corresponding to the same dumbbell-shaped configuration of two alpha particles, as shown in figure 2. A similar configuration of three alpha particles has been proposed for the 7.65 MeV 0^{+} state in ^{12}C which also has an extremely large reduced α decay width. In fact, Morinaga (1966) and Ikeda *et al* (1968) proposed that such highly clustered states might be a general feature in light nuclei, occurring at excitation energies close to the threshold for break-up into the constituent α-clusters. It was expected, however, that in heavier nuclei, as the energy of the break-up threshold increased, strong mixing of the cluster states with the much more numerous, less exotic, states at these high excitation energies, would result in their significant broadening. The consequence of this mixing and associated broadening is twofold. First, the increased width makes the experimental observation of these states as resonances more difficult and, second, the expected strong mixing would call into question the usefulness of the cluster basis as an approximate solution to the full nuclear Hamiltonian.

Surprisingly, therefore, in some of the very first studies of the energy dependence of the scattering of heavy ions—$^{12}\mathrm{C} + {}^{12}\mathrm{C}$—sharp structures were observed corresponding to narrow resonances at high excitation energy in the composite nucleus ^{24}Mg. It was suggested immediately that these resonances might correspond to molecule-like configurations of two ^{12}C nuclei. Subsequent studies have demonstrated the existence of similar phenomena in a wide range of nuclear systems up to $^{28}\mathrm{Si} + {}^{28}\mathrm{Si}$.

The interpretation of these observations in terms of the molecular concept has frequently been quite controversial and, even at the time of writing, it is fair to say that there is no one piece of evidence which unequivocally points to the validity of this interpretation. The body of evidence does, however, strongly point to the essential correctness of this idea.

In this review we briefly summarize the vast body of experimental results in this area

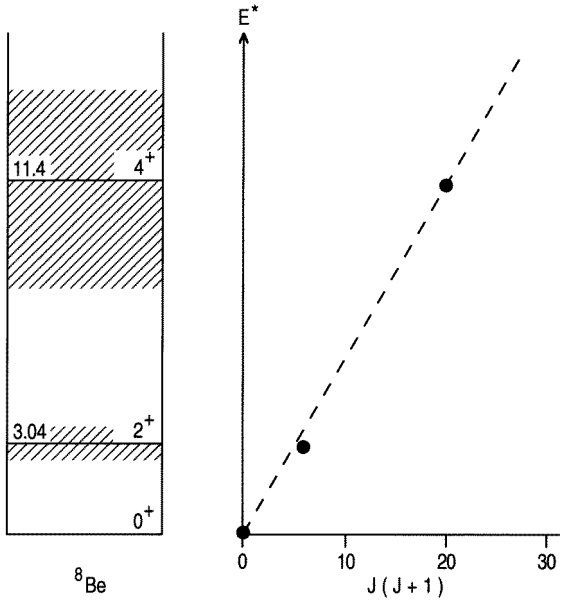

Figure 2. Energy level diagram for ^{8}Be showing the expected rotational sequence for an α–α molecule.

and also discuss the essential theoretical ideas. For more information, the interested reader is directed to a number of other recent reviews, conference proceedings and books (Erb and Bromley 1985, Fulton and Rae 1990, Wuosmaa *et al* 1995, Freer and Merchant 1997, Kyoto 1988, Turku 1992, Santorini 1994, Strasbourg 1994, Greiner *et al* 1995). Finally, we address the future possibilities of research on nuclear molecules and suggest some possible new avenues for experimental investigation.

2. Review of experimental results

2.1. Early experiments

The first indications of the existence of nuclear molecular states came from a series of experiments carried out at Chalk River in the early 1960s by Bromley and collaborators. These experiments exploited the, then newly available, high energy-definition, beams of ^{12}C and ^{16}O and used, also recently developed, silicon surface barrier detectors. Data for the energy dependence of elastic scattering of ^{12}C+ ^{12}C and ^{16}O+ ^{16}O, measured at a centre-of-mass scattering angle of 90°, are shown in figure 3 (Bromley *et al* 1960). At low energies, the data for both systems show an E^{-2} dependence characteristic of pure Coulomb (Mott) scattering of two identical nuclei. For the ^{12}C + ^{12}C system, however, at centre-of-mass energies above 6.5 MeV, the data show evidence for a number of structures, some of which are quite narrow. In the energy range covered by these measurements, the ^{16}O + ^{16}O data show a rather smooth behaviour, the fall-off from the E^{-2} behaviour arising from the strong absorption of the projectile expected in the close, head-on collisions which occur at the higher energies. From these data and measurements of the angular dependence of the elastic scattering cross section, it was not possible to say definitively whether or not the energy-dependent structures in the ^{12}C + ^{12}C system arise from isolated resonances. Nevertheless,

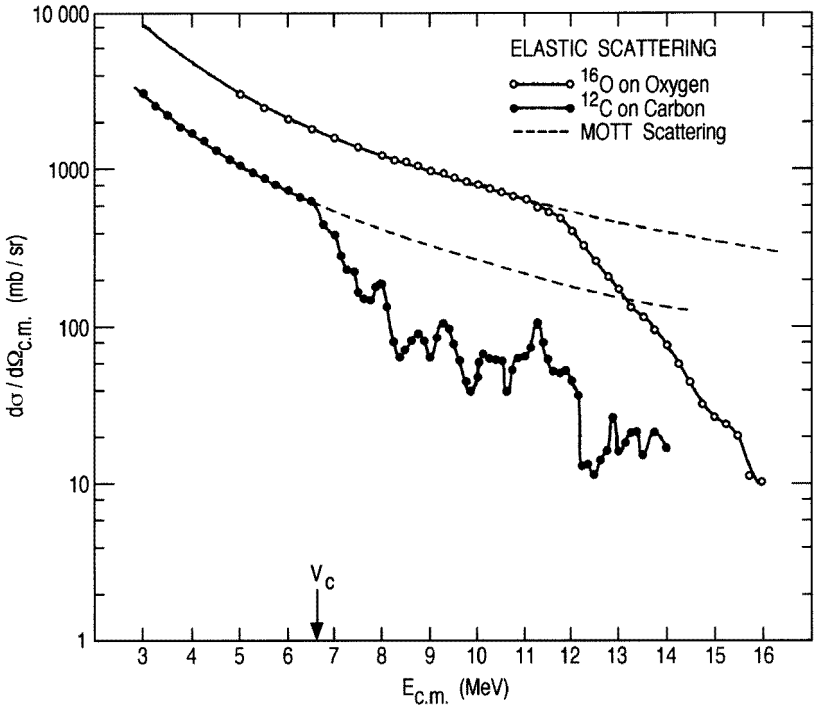

Figure 3. Excitation function data at $\theta_{cm} = 90^\circ$ for $^{12}C + {}^{12}C$ and $^{16}O + {}^{16}O$ elastic scattering (Bromley *et al* 1960).

the compelling suggestion that the observed structures represented the excitation and decay of molecule-like degrees of freedom was made. At the same time, it was noted that the absence of structure in $^{16}O + {}^{16}O$ scattering presented a challenge to any explanation.

Further measurements of reaction channels for $^{12}C + {}^{12}C$ and $^{16}O + {}^{16}O$, carried out shortly thereafter, revealed a similar pattern. The data (Almqvist *et al* 1960, Bromley *et al* 1961) for $^{12}C + {}^{12}C$ are shown in figure 4. In addition to structures similar to those observed in the elastic scattering data, at energies below 6.5 MeV, a number of extremely narrow resonances were seen, strongly correlated in the different reaction channels. As was the case for elastic scattering, the reaction data for $^{16}O + {}^{16}O$ showed only a relatively smooth energy dependence. Of particular note in the $^{12}C + {}^{12}C$ reaction data is the low energy at which the narrow resonances were observed—below the energy (V_C) corresponding to the Coulomb repulsion of two spherical ^{12}C nuclei. It was therefore suggested that these resonances may correspond to extremely deformed configurations of the combined system which could result in a scattering potential which displays a pocket at large radial separation as indicated in figure 5. The observed resonances would then correspond to the quasi-bound states in this secondary minimum, the inner barrier of which would prevent their immediate dissolution into the compound nucleus, and thus account for their narrow widths. Indeed, further analysis of the elastic scattering and reaction data showed that the resonances did indeed have extremely large partial widths for decay into $^{12}C + {}^{12}C$, as expected for such molecule-like configurations. It should, however, be emphasized that, at that time, no theoretical basis existed for nuclear structure effects which might produce the postulated quasi-stable molecular configurations.

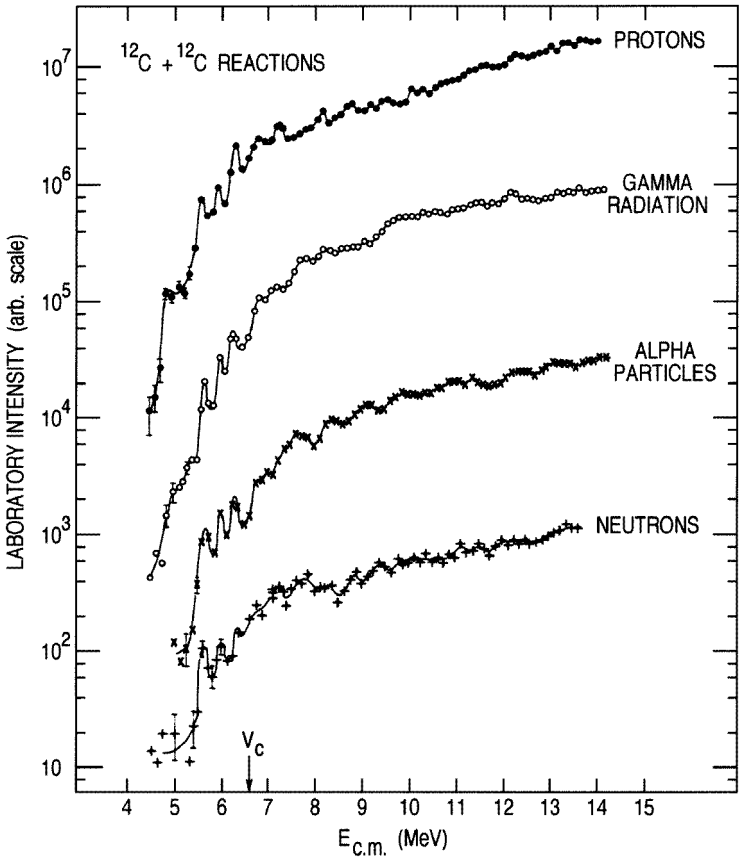

Figure 4. Reaction cross section data for $^{12}C + ^{12}C$ (Almqvist *et al* 1960) as a function of centre-of-mass bombarding energy. The arrow indicates the expected Coulomb barrier (V_C) for spherical ^{12}C nuclei.

2.2. Barrier resonances in reaction channels

Following the initial observation of resonant behaviour in the elastic scattering of $^{12}C + ^{12}C$ at energies very close to the Coulomb barrier, a variety of other more detailed studies were performed. Of particular interest were reaction channels leading to final states such as $^{12}C(^{12}C, \alpha)^{20}Ne$ or $^{12}C(^{12}C, p)^{23}Na$. Galster *et al* (1977) and Voit *et al* (1977) reported detailed excitation-function data for the $^{12}C(^{12}C, \alpha)$ reaction populating several levels in ^{20}Ne, spanning centre-of-mass energies between 4 and 13 MeV. Many resonances were observed, and by measuring the angular distribution of transitions to either 0^+ or 2^- final states (see section 2.5), spins were assigned to 11 of these resonances. The non-statistical origin of these resonances was demonstrated by their correlated appearance in the excitation functions for many different channels.

These narrow resonances were also studied in inclusive gamma-ray measurements. Kettner *et al* (1977) determined the energy dependence of the total $^{12}C + ^{12}C$ reaction cross section at centre-of-mass energies between 2.9 and 6.2 MeV by measuring the inclusive yield of gamma rays from the alpha, proton, and neutron evaporation channels leading to ^{20}Ne, ^{23}Na and ^{23}Mg, respectively. These measurements were extended to higher energies

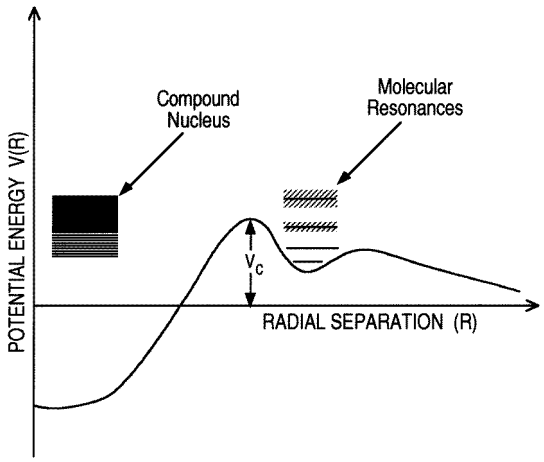

Figure 5. Schematic ion–ion potential suggested to give rise to the low-energy ($E < V_C$) $^{12}C + {}^{12}C$ resonances.

by Andritsopoulos *et al* (1980) and Erb *et al* (1980), who confirmed the existence of the quasi-molecular resonances observed previously, and also identified a number of new levels.

The richness of the experimental spectrum is demonstrated in figure 6 taken from Erb and Bromley (1985), where the smooth energy dependence of the cross section on penetrability factors has been divided out, producing the so-called nuclear structure factor. In total, 20 or more narrow resonances are seen, with total widths ranging from about 100–200 keV in the centre of mass. The spin assignments in figure 6 are taken primarily from the $^{12}C(^{12}C, \alpha)$ work described above. The lifetimes of these resonances are of the order 10^{-21} s, corresponding to the time of a few rotations of the $^{12}C + {}^{12}C$ system. Moreover, as before, these states also possess large values of the partial width for decay into $^{12}C + {}^{12}C$, consistent with a quasi-molecular interpretation for these resonances. Interestingly, the broad structures observed in earlier $^{12}C + {}^{12}C$ elastic scattering data were not seen in these reaction channels, suggesting that the potential scattering picture used to describe the elastic scattering data was not applicable in this case. Furthermore, as was the case for the narrow states observed in elastic scattering near the Coulomb barrier, similar structure was almost completely absent in corresponding excitation function curves for $^{16}O + {}^{16}O$ scattering, as shown by Spinka and Winkler (1972, 1974).

2.3. Elastic scattering at high energies

With the availability of accelerators capable of producing beams with higher energies, studies of elastic scattering of the various systems which had initially inspired the greatest interest were pushed to energies far above the Coulomb barrier. In these new measurements, additional interesting new features were observed. In many respects these were qualitatively similar to the resonances observed in the barrier region.

In the $^{16}O + {}^{16}O$ case (figure 7), in contrast to the rather featureless behaviour of the excitation function at Coulomb barrier energies, data obtained by Siemssen *et al* (1967), Maher *et al* (1969) and Halbert *et al* (1974) at higher energies displayed pronounced, regular oscillations, 1–2 MeV in width, which were accompanied by narrower features. These broad structures were found to be a rather common feature in the elastic scattering of many other systems of identical light nuclei and, instead of quasi-molecular behaviour,

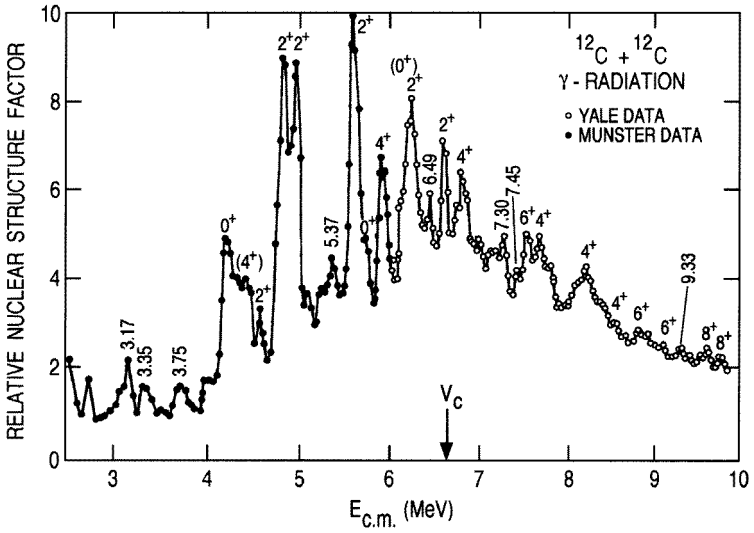

Figure 6. Deduced nuclear S factor for the $^{12}C + {}^{12}C$ total reaction cross section (Erb and Bromley 1985).

were thought to reflect the properties of the underlying optical potential. Each cross section enhancement appeared to arise from an angular momentum window, which was characterized by a partial wave close to the so-called grazing value—so named because classically this value corresponds to the angular momentum obtained for collisions between two touching spheres. This picture was supported by the finding of Maher *et al* (1969) that the optical potential needed to describe the data was considerably shallower than that usually applied to scattering in these light systems. This small depth, combined with the possibility of a repulsive core, suggested that Pauli exclusion effects might be important for collisions where the nuclei have significant overlap. Note that for identical spin zero systems such as $^{12}C + {}^{12}C$ and $^{16}O + {}^{16}O$ only even values of the relative angular momentum are allowed.

Similar gross-structure oscillations were observed in $^{12}C + {}^{12}C$ elastic scattering at higher energies, as demonstrated by Reilly *et al* (1973) and Wieland *et al* (1976), also shown in figure 7. Between 15 and 40 MeV, these oscillations, as was the case in the $^{16}O + {}^{16}O$ system, followed the behaviour expected for the opening of a series of l windows, and were separated by the energy expected for the sequence of grazing partial waves in this system. Narrower, intermediate width features, considerably more prominent than those in the $^{16}O + {}^{16}O$ system, also persisted. It was suggested that these intermediate width peaks might represent some fragmentation of the strength for each successive partial wave, which, due to structural considerations, might be enhanced in the $^{12}C + {}^{12}C$ system relative to $^{16}O + {}^{16}O$.

A curious middle ground was found in the scattering of $^{12}C + {}^{16}O$, as measured by Malmin *et al* (1972) and Stokstad *et al* (1972) shown in figure 8. In this system, little evidence was seen of regular gross-structure oscillations. This was believed to be due to the fact that, with non-identical particles, both odd and even partial waves can participate. In identical particle systems the widths of the gross structures tend to be of the order of 2–3 MeV, a value comparable to the expected energy spacing between adjacent partial waves in the $^{12}C + {}^{16}O$ systems. Hence, in the non-identical particle case, the enhancements in the

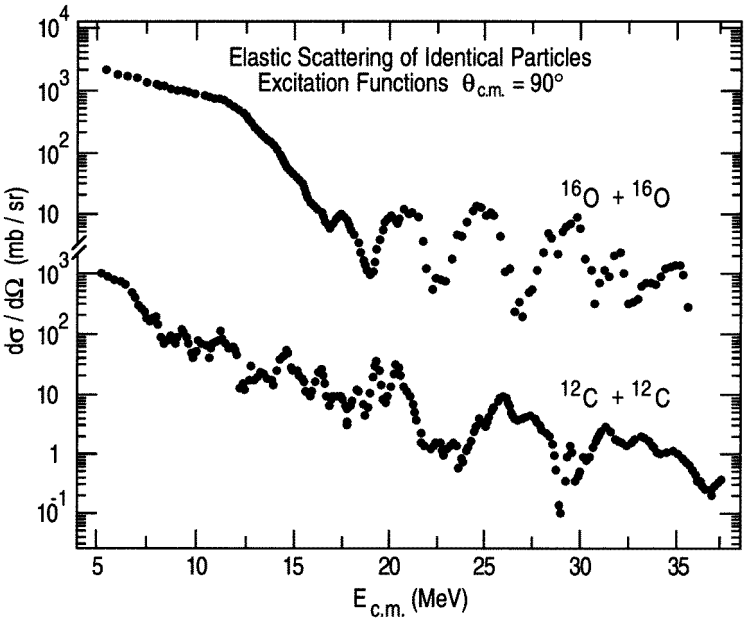

Figure 7. Elastic scattering excitation functions at $\theta_{\rm cm} = 90^\circ$ for $^{12}{\rm C} + {}^{12}{\rm C}$ (Reilly *et al* 1973, Wieland *et al* 1976) and $^{16}{\rm O} + {}^{16}{\rm O}$ (Siemssen *et al* 1967, Maher *et al* 1969).

cross section from successive partial waves most likely overlap and wash out the regular structure. Intermediate width or narrow structures, however, are still apparent. An example is a strong resonance observed at a centre-of-mass energy of 19.7 MeV, with an assigned spin of 14^+. The narrow width of this structure (300 keV), as with the barrier resonances at lower energies, corresponds to a lifetime which is long compared to the nuclear transit time, and supports the interpretation of this resonance as a molecular state.

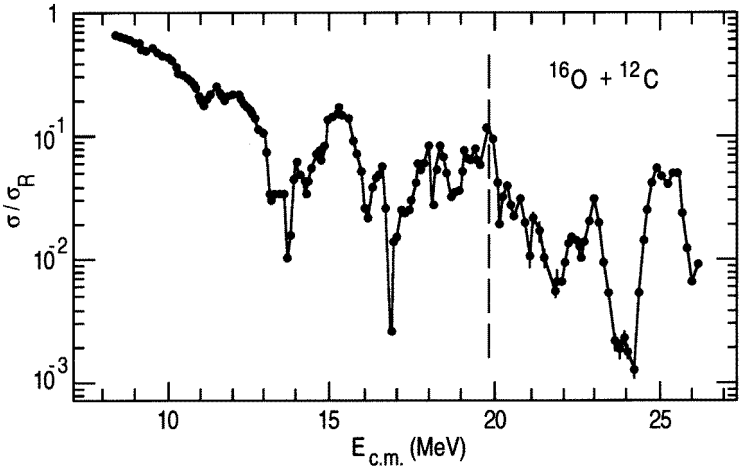

Figure 8. Elastic scattering excitation function at $\theta_{\rm cm} = 90^\circ$ for $^{12}{\rm C} + {}^{16}{\rm O}$ (Malmin *et al* 1972, Stockstad *et al* 1972).

2.4. Resonances in fusion and inelastic scattering

Broad structures reminiscent of those observed in elastic scattering at higher bombarding energies have been seen in the energy dependence of the total fusion cross section for a number of heavy-ion systems (Sperr *et al* 1976a, b, Kovar *et al* 1979). Examples are shown in figure 9. Fusion is defined as the cross section for production of the compound nucleus formed by complete amalgamation of the target and projectile nuclei and is measured either by direct detection of the residual nuclei produced following evaporation of nucleons or alpha particles from the compound nucleus or by detection of gamma rays from their subsequent de-excitation. The correlation between the broad structures in the fusion and those in the elastic scattering channel is quite striking, the width and spacings being quite similar. This relationship is obvious in the simplest potential scattering picture of the broad structures in elastic scattering as, in this case, the width of the resonances arises from the coupling of the potential resonances to the compound nucleus described by the imaginary part of the optical model potential or penetration of the wavefunction through the inner barrier of a two-humped potential. The strength of this coupling is reflected by the large cross sections associated with the fusion structures which represent a significant fraction of the unitary limit for successive partial waves corresponding to grazing collisions of the two nuclei.

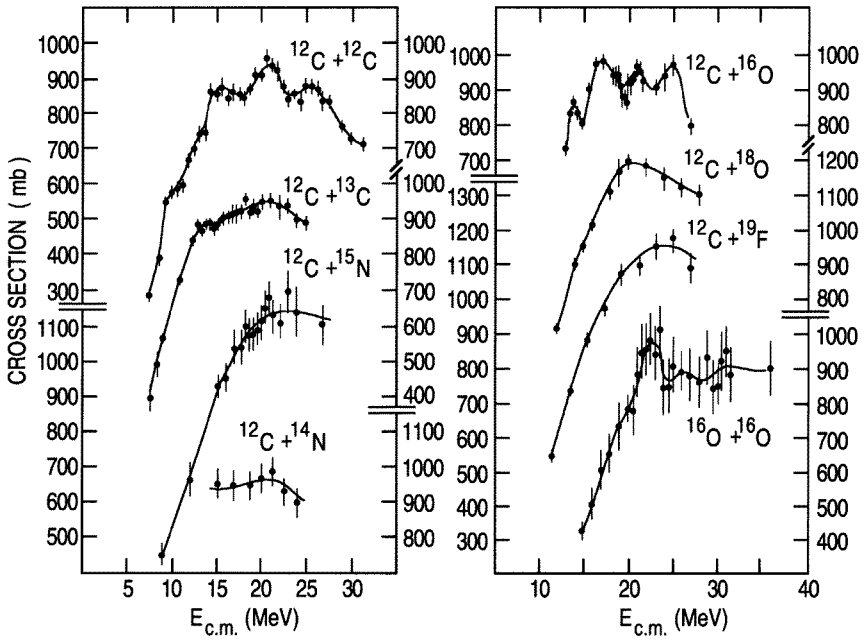

Figure 9. Total fusion cross section excitation functions for a number of heavy-ion systems.

Strong broad structures similar to those seen in the fusion cross sections have also been observed in inelastic scattering reactions for heavy-ion systems such as $^{12}C + ^{12}C$ where one or both nuclei are excited. The first examples (Cormier *et al* 1977, 1978) of such data are shown in figure 10 which displays the energy dependence of the cross section for both single and double inelastic excitation of $^{12}C + ^{12}C$ to the 4.43 MeV $J^{\pi} = 2^{+}$ level. For comparison, the fusion cross section for $^{12}C + ^{12}C$ is also shown. These data are particularly important in view of theoretical suggestions relating to the crucial role played by inelastic

excitation in coupling potential scattering resonances to the intrinsic degrees of freedom of the colliding nuclei (see section 3.3). The total cross sections associated with the inelastic channels are the dominant fraction of the unitary limit for the partial wave associated with each structure which indicates the necessity of including these reaction channels explicitly in any theoretical description and not simply treating them as perturbations to the elastic scattering channel.

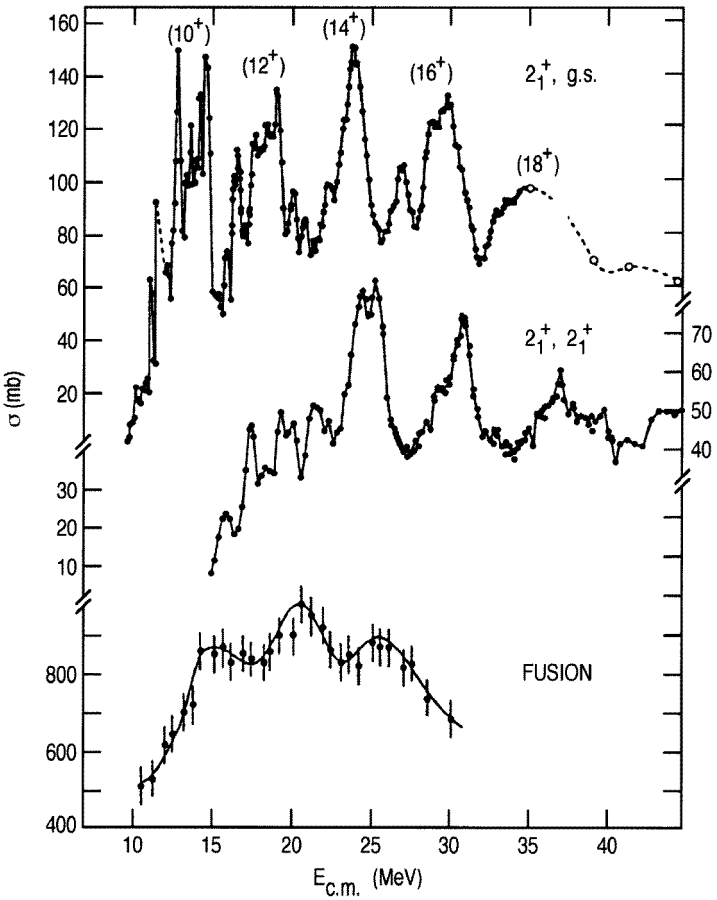

Figure 10. Energy dependence of the cross section for single (2_1^+, g.s.) and double (2_1^+, 2_1^+) excitation of $^{12}C + {}^{12}C$ (Cormier *et al* 1977, 1978). Also shown is the $^{12}C + {}^{12}C$ fusion cross section.

2.5. Spin assignments and resonance spectroscopy

Spin assignments (for resonances) are crucial in order to perform comparisons of the spectroscopy of the observed molecular resonances with the predictions of various models. A variety of techniques have been used over the past three decades to determine the spins of resonances in scattering and reaction channels. These include phase shift analyses, angular distribution measurements, and studies of the angular correlation between scattered heavy ions and either particles or gamma rays emitted from the decay of excited states in the participating nuclei.

2.5.1. Phase shift analyses and elastic scattering resonances. Phase shift analyses have been applied to detailed elastic scattering angular distribution data in attempts to identify resonances from the characteristic energy dependence of the scattering matrix elements expected for a resonant channel. An excellent example of this method is due to Korotky *et al* 1979, who analysed several precisely measured $^{12}C + {}^{12}C$ elastic scattering angular distributions at centre-of-mass energies between 6.5 and 6.9 MeV (figure 11(a)). The deduced scattering matrix parameters are shown in figure 11(b), and are consistent with spin assignments of 2^+ and 4^+ for resonances at $E_{cm} = 6.64$ and 6.83 MeV, respectively. With these spin assignments, the ^{12}C reduced widths could then be precisely determined, and these reflect a large $^{12}C + {}^{12}C$ parentage consistent with the expectations for a quasimolecular state.

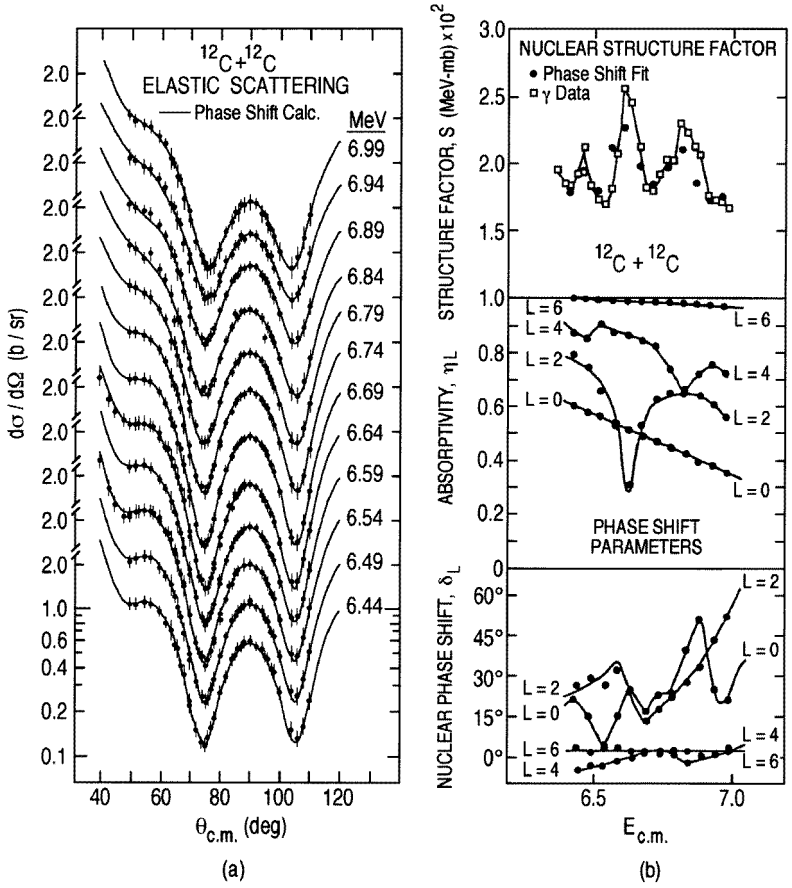

Figure 11. (a) Detailed elastic scattering angular distributions for $^{12}C + {}^{12}C$ at energies near the Coulomb barrier. (b) Phase shifts (δ_L), absorption (η_L) and nuclear structure factors (S) deduced from these data (Korotky *et al* 1979).

Care must be taken, however, in extracting such information from elastic scattering data. Near the barrier, Coulomb effects dominate and deviations due to nuclear processes in the scattering are generally small. Hence, data of excellent quality are required. At higher energies, many more partial waves contribute and the resonant amplitude interferes not only with the Coulomb scattering, but with contributions from direct nuclear scattering.

The effect that a resonance has on the elastic-scattering angular distributions may therefore often be difficult to disentangle.

2.5.2. Rearrangement reactions. A similar approach has been applied to angular distribution data for rearrangement or transfer reactions, which have the advantage that they may be less sensitive to Coulomb interference effects and direct reaction amplitudes. One example which has received much attention is the ^{12}C(^{12}C, α)^{20}Ne reaction. For the ground-state transition, where all nuclei have zero spin, the angular distribution may be fit to Legendre polynomials. If a single resonance dominates the reaction amplitude, the angular distribution will be well described by $\sigma(\theta_{\rm cm}) \approx (P_l(\cos\theta_{\rm cm}))^2$. The situation, however, usually is more complicated and many partial waves may participate in the reaction. In this case, the measured angular distribution may then be fit to the expression $\sigma(\theta) = |\Sigma B_l P_l(\cos\theta)|^2$, where B_l are complex parameters representing the amplitude of each partial wave. Figure 12 shows an example of such data and a corresponding fit from Basrak *et al* (1976), for a spin-6 resonance in the ^{12}C + ^{12}C system at $E_{\rm cm} = 7.53$ MeV. Comprehensive data of this type have also been reported by Erb *et al* (1976). This technique has also been applied to other transfer or rearrangement reactions leading to spin-zero exit channels in which resonances are observed, as demonstrated for example, by Hurd *et al* (1980) who studied the ^{12}C(^{16}O, ^{8}Be)^{20}Ne ground-state (g.s.) reaction between $E_{\rm cm} = 11.5$ and 18.6 MeV.

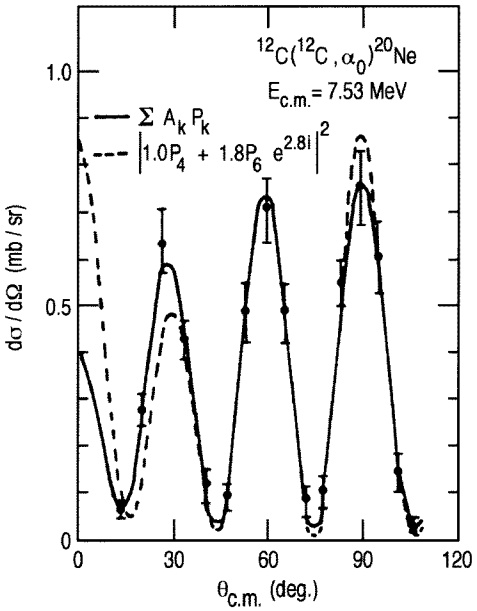

Figure 12. On resonance angular distribution for the ^{12}C(^{12}C, α)^{20}Ne(g.s.) reaction (Basrak *et al* 1976). The fits imply a resonance spin of 6.

Angular distributions of transitions to unnatural parity states in the residual nucleus have also been used to restrict the possible spin values of resonances in the ^{12}C(^{12}C, α)^{20}Ne reaction. Following Almqvist *et al* (1963), Galster *et al* (1977) analysed the angular distributions of alpha particles from the transition to the 2^- state in ^{20}Ne. Here, selection rules require that for a given partial wave l in the entrance channel only two l values,

$l_{out} = l_{in} \pm 1$, can contribute to the cross section in that exit channel. In the case of a single dominant l the angular distribution is again expressed in terms of Legendre polynomials. Using this method, the spins of several resonances near the Coulomb barrier were determined which, in general, agreed with those obtained with other techniques.

2.5.3. Angular-correlation techniques. In many cases, particularly at energies substantially above the Coulomb barrier, resonances are observed in inelastic scattering channels where the resulting final state spin is not zero. As a result, angular distribution measurements of the type outlined above lose their sensitivity to the angular momenta involved and, in general, cannot be used to assign J^{π} values. Information about the dominant angular momenta can, however, be recovered by detecting the radiation emitted in the decay of the excited state in the scattered nucleus in coincidence with the scattered particle. These angular correlation techniques can, in addition to resonance spins, provide information about the reaction mechanism through the determination of magnetic substate populations and spin alignments. The general formalism for the analysis of particle–gamma-ray angular correlation data has been outlined by, for example, Ferguson (1965), Rybicki *et al* (1970) and Satchler (1983).

2.5.4. Particle–gamma-ray angular correlations. Early examples of particle–gamma-ray angular correlation measurements applied to inelastic scattering resonances include the work of Cannell *et al* (1979) and Jachcinski *et al* (1979), who studied the inelastic scattering of $^{12}C + {}^{12}C(2^+)$ and $^{12}C + {}^{16}O(2^+, 3^-)$, respectively, by detecting the scattered heavy ions at several angles, and the de-excitation gamma rays at a single angle using a NaI detector. Inelastic scattering data from Cannell *et al* (1979) appear in figure 13, which shows the particle angular distribution measured in coincidence with gamma rays, taken at several beam energies.

In the $^{12}C + {}^{12}C$ case, Cannell *et al* found that slightly better fits to the correlation data could be obtained with a distorted-wave description of the reaction, and the suggestion was made that both the excitation function and angular correlation data for the $^{12}C + {}^{12}C(2^+)$ channel could be explained without resorting to the concept of quasi-molecular resonances. Fits assuming isolated resonances with spins consistent with earlier assignments (the dashed curve in figure 13) were, however, still in reasonable agreement with the data.

In the $^{12}C + {}^{16}O$ case, resonances between 19 and 25 MeV in the centre-of-mass system have been studied using the direct gamma-ray detection method by Jachcinski *et al* (1979), and a technique employing the analysis of Doppler broadened line shapes by Beene *et al* (1980). In each case, again the results were not fully conclusive. While, for some of the resonances which were studied, the data were consistent with spin assignments obtained from other techniques, the results of both measurements indicated that the situation in this system was more complicated than that of a simple rotational sequence based on a quasi-molecular configuration. Similar line-shape measurements have been applied to the $^{12}C + {}^{12}C$ system by Sugiyama *et al* (1985).

An extension of the particle–gamma-ray angular correlation technique became possible with the advent of large solid-angle NaI detector arrays, or 'crystal balls'. The Munich group, who had previously used single NaI detectors in conjunction with silicon particle detectors to study the spin alignment in $^{12}C + {}^{12}C(2^+)$ inelastic scattering (Trombik *et al* 1984), employed a combination of silicon surface-barrier particle detectors and a 162 element NaI array to determine correlated spin alignments for resonances observed in $^{12}C(2^+) + {}^{12}C(2^+)$ mutual inelastic scattering (Konnerth *et al* 1985). They determined

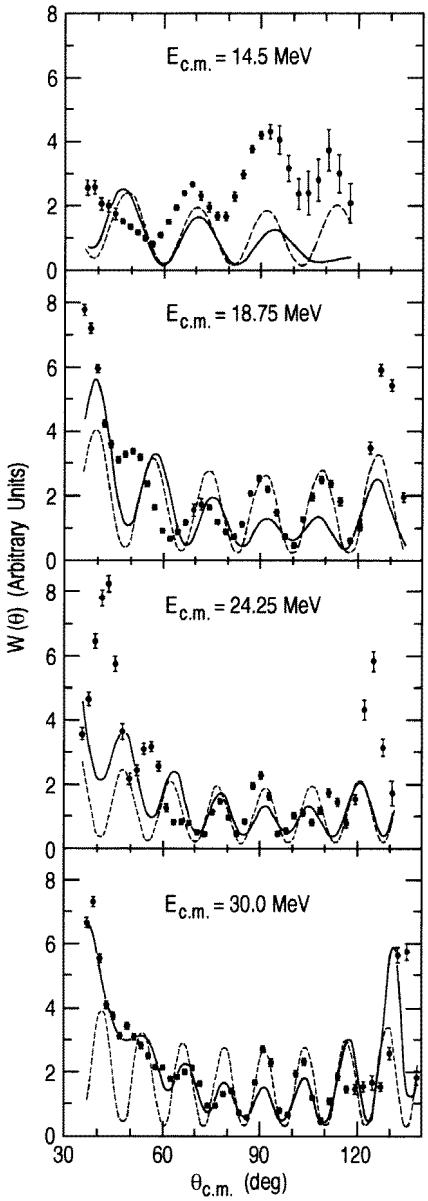

Figure 13. ^{12}C–^{12}C–γ angular correlation data (Cannell *et al* 1979). The full curves are distorted wave Born approximation fits and the dashed curves represent the expectations for isolated resonances.

that, in the energy region of a resonance, the spins of the two inelastically excited ^{12}C nuclei were preferentially aligned with the orbital angular momentum consistent with the expectations for an orbiting molecular configuration of two oblate ^{12}C nuclei.

In another set of experiments using a large NaI array coupled with particle detectors, the Pennsylvania group studied resonances in two systems, ^{16}O + ^{16}O (Pate *et al* 1990), where gross structures are present in the 3^- excitation function between centre-of-mass

energies of 25 and 40 MeV, and $^{24}Mg + {}^{24}Mg$ (Wuosmaa *et al* 1987a, 1990), where an intriguing series of very sharp resonances appears in a large number of inelastic scattering channels at energies between 40 and 50 MeV. The 4-π gamma-ray acceptance afforded by the spin spectrometer (Jääskaleinen 1983) allowed a full magnetic substate decomposition of the inelastic scattering cross section for inelastic scattering to the first excited 2^+ state in ^{24}Mg, and the excited 3^- state in ^{16}O. For the sharp resonances in $^{24}Mg + {}^{24}Mg$ inelastic scattering, the magnetic-substate angular distributions proved quite sensitive to the resonance behaviour in that system, and suggested spin assignments from 36 to $40\hbar$ in the energy range $E_{cm} = 45$–55 MeV. The extracted spin sequence and the average spacing of the resonances were consistent with a shape which strongly resembled two ^{24}Mg in a pole-to-pole grazing configuration. For the $^{16}O + {}^{16}O$ system, the results were more ambiguous. The data for one resonance at $E_{cm} = 28.1$ MeV firmly suggested a spin of 20. At higher energies, while unambiguous assignments could not be made, the results strongly indicated that the dominant angular momenta did not follow a simple rotational sequence, and furthermore were inconsistent with the values expected from band-crossing model calculations.

2.5.5. Particle–particle angular correlations. Similar methods have been applied to particle-decaying final states excited in inelastic scattering reactions. Rae *et al* (1987a, 1987b) have performed alpha-particle coincidence measurements designed to extract spins for resonances in $^{12}C + {}^{12}C$ scattering from the $^{12}C(^{12}C, \alpha\alpha)^{16}O$ reaction. Here, the primary reaction is $^{12}C(^{12}C, \alpha)^{20}Ne^*$, where the residual ^{20}Ne nucleus is left in an excited state above its alpha-particle decay threshold of 4.73 MeV. The correlation between the alpha particle from the decay of the excited ^{24}Mg compound nucleus and the alpha particle from the decay of the excited ^{20}Ne is quite sensitive to the spin of the compound nucleus. This technique was successfully employed to measure spins of several resonances between 19 and 27 MeV centre-of-mass energy, as shown in figure 14. The spin assignments thus obtained were consistent with those determined from other techniques. The same method was used by Rae *et al* (1987b) to examine the $^{12}C(^{12}C, {}^{8}Be)^{16}O(\alpha)$ reaction, again yielding a spin assignment consistent with previous work. The various spectroscopic data obtained using these techniques were used in attempts to classify resonances according to a variety of schemes deduced from theory or from semi-empirical models.

2.6. Resonances in heavier asymmetric systems

Following the early work, it was assumed that molecular resonances were confined to the $^{12}C + {}^{12}C$, $^{12}C + {}^{16}O$ and $^{16}O + {}^{16}O$ systems. It was expected that for heavier systems the increased number of reaction channels and increased level density in the compound nucleus would result in an enormous broadening of the molecular resonances and thus make them essentially unobservable. The first evidence that this was not the case came from measurements (Braun-Münzinger *et al* 1977) of the large-angle elastic scattering of $^{16}O + {}^{28}Si$, the angular distribution of which shows a remarkable rise at backward angles, far in excess of expectations based on optical model calculations. These results are shown in figure 15. The data at forward angles show the usual behaviour for such systems: a rise above the Rutherford value at the grazing angle, arising from diffractive effects, and a steep fall-off at larger angles corresponding to strong absorption of smaller impact parameter collisions. Rather than continuing to larger angles, this fall-off is interrupted by the onset of oscillatory behaviour and a rise at 180°. The period of the angular oscillations corresponds, in this case, to an angular momentum of $26\hbar$, close to the grazing value for this bombarding energy.

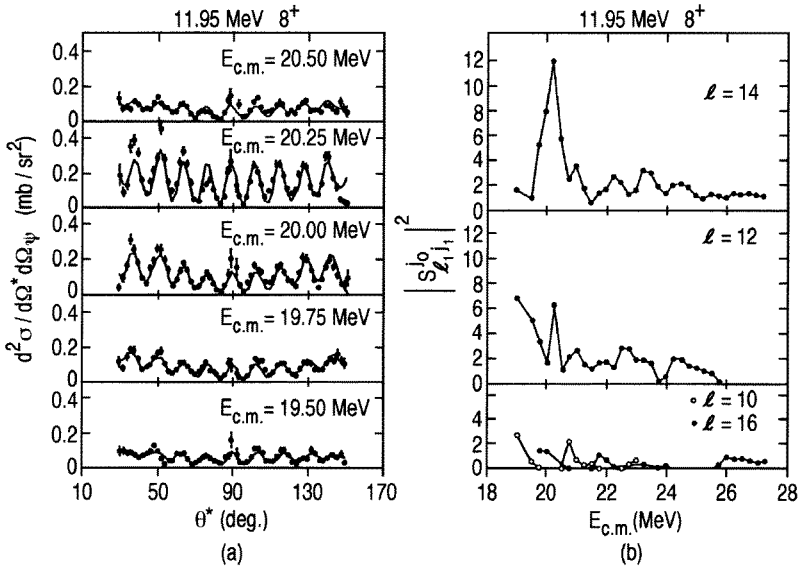

Figure 14. (a) Correlation data for $^{12}C(^{12}C, \alpha\alpha)^{16}O$ from Rae *et al* (1987a). (b) Energy dependence of the deduced scattering matrix elements.

The energy dependence of the cross section for elastic and inelastic scattering of $^{16}O + {}^{28}Si$ measured at $\theta_{cm} = 180^\circ$ is shown in figure 16 (Barrette *et al* 1978). These data display a number of broad (1–2 MeV) wide structures correlated between the two channels but showing no regular pattern with energy.

Similar behaviour has been reported for scattering and reactions with ^{12}C and ^{16}O projectiles incident on ^{24}Mg and ^{28}Si (Clover *et al* 1978, Kubono *et al* 1979a, Paul *et al* 1978, Sanders *et al* 1980). A particularly interesting result was found for the large-angle scattering of $^{12}C + {}^{28}Si$ which showed that the backward angle enhancement was not only a feature of the elastic scattering and low-lying inelastic scattering channels but was a feature of essentially all reaction channels (Shapira *et al* 1979). This result suggested that, for these heavier systems, the backward-angle yield resulted from the decay of an extended, equilibrated di-nuclear system. The average energies of the emitted fragments were found (Shapira *et al* 1982) to be consistent with complete damping of the entrance channel energy, the final state energies being consistent with the Coulomb repulsion plus rotational energy of the di-nuclear complex.

2.7. Resonances in the heaviest systems

The search for resonance phenomena has been extended to a number of heavier systems. A study (Kubono *et al* 1979b) of the large-angle elastic scattering of $^{16}O + {}^{40}Ca$ showed an energy dependence with the same general features as for $^{16}O + {}^{28}Si$ but with a cross section one to two orders of magnitude smaller. Much more detailed studies (Betts *et al* 1979, 1981a, b, Betts 1984a, Zurmühle *et al* 1983, Kutt *et al* 1985, Saini *et al* 1987, Wuosmaa *et al* 1987b) of a number of heavier, symmetric and near symmetric systems has, however, revealed a much richer structure. An angular distribution (Betts 1984a) for the elastic scattering of $^{28}Si + {}^{28}Si$ at an energy of 120 MeV is shown in figure 17. As was the case for the lighter systems, the behaviour at angles forward of 50° is well described by

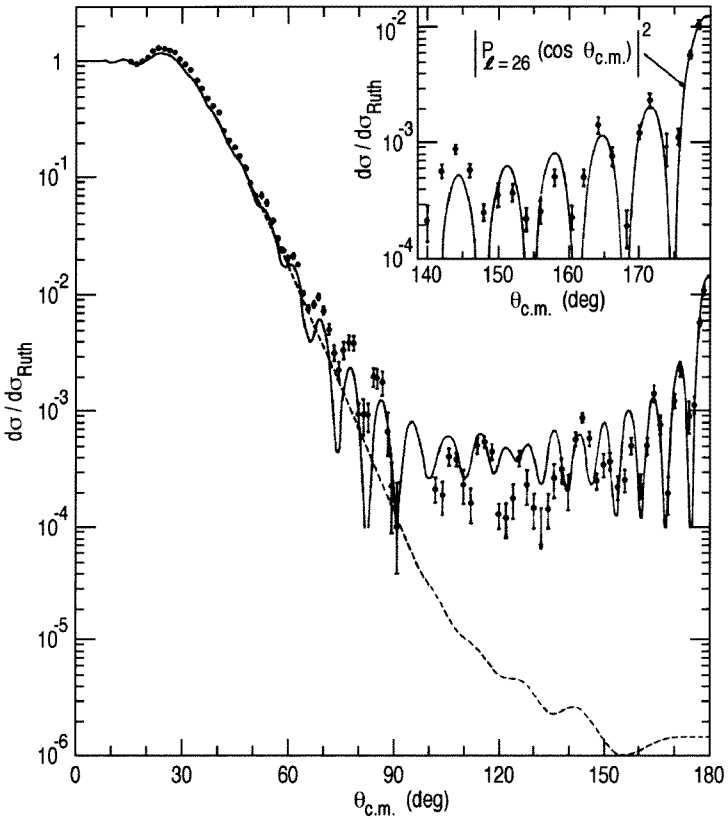

Figure 15. Angular distribution for elastic scattering of $^{16}O + {}^{28}Si$ at $E_{LAB} = 55$ MeV (Braun-Münzinger *et al* 1977). The dashed curve is the result of an optical model calculation.

the results of calculations using the optical model (full curve). At larger angles, however, the data show an oscillatory pattern characteristic, in this case, of an almost pure $P^2_{40}(\cos\theta)$ behaviour. Even more striking, the energy dependence of the cross section (Betts *et al* 1981b, Betts 1984a) integrated over the angular region 60°–90° shows not only a series of broad structures, each of which is characterized by the indicated angular momentum, but also a fragmentation of these structures into very narrow (∼100 keV) wide resonances as shown in figure 18. Also shown in figure 18 is the summed yield of all inelastic scattering channels in the angular range 60°–90° as a function of energy. The structure in the total yield correlates strongly with that observed in the elastic scattering channel and it has been concluded, based on an extensive statistical analysis of these data (Saini and Betts 1984), that the observed narrow structures do indeed correspond to isolated resonances with angular momenta of order $40\hbar$ lying at excitation energies near 70 MeV in the compound nucleus ^{56}Ni.

Another interesting feature of these data is shown in figure 19 which displays the average large-angle differential cross section summed over all inelastic scattering channels for the $^{28}Si + {}^{28}Si$, $^{28}Si + {}^{30}Si$ and $^{30}Si + {}^{30}Si$ systems (Betts 1984a). For the latter two systems, the prominent structures observed in the $^{28}Si + {}^{28}Si$ system have completely disappeared. This disappearance of the structure is also accompanied by a reduction in the overall magnitude of the cross section by a factor of two for each addition of a pair of neutrons to the

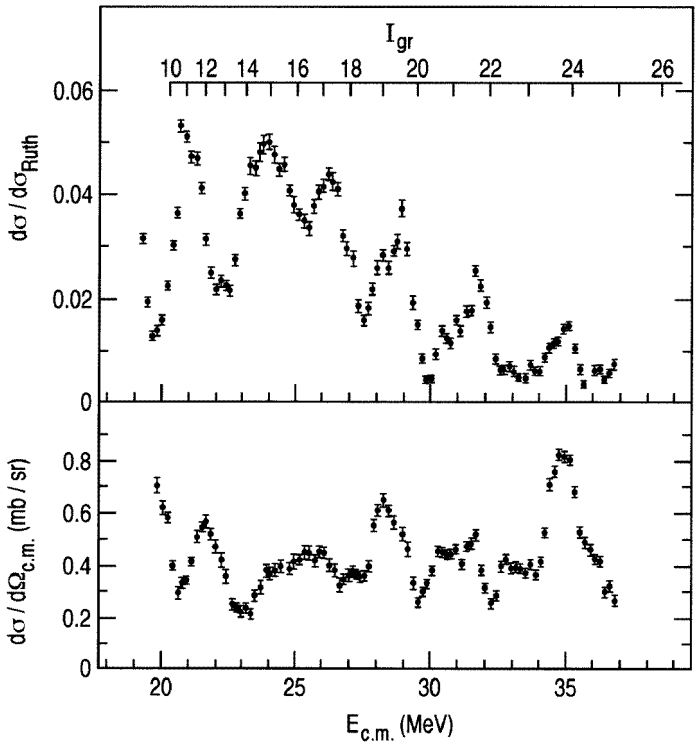

Figure 16. Excitation function for $\theta_{cm} = 180^{\circ}$ elastic (upper) and inelastic (lower) scattering of $^{16}O + {}^{28}Si$ (Barrette *et al* 1978).

system. Detailed studies of the elastic scattering of these systems (Betts 1984b) led to the conclusion that the overall features of the optical model required to describe the scattering process are almost identical. This observation suggests that the large-angle enhancement, and the energy-dependent structure therein, be described by some features of the composite system rather than any properties of the scattered nuclei which, in the case of ^{28}Si and ^{30}Si, are very similar anyway.

The most striking example of resonance behaviour in these heavy systems is for $^{24}Mg + {}^{24}Mg$, data for which is shown in figure 20. These data (Zurmühle *et al* 1983, Wuosmaa *et al* 1987a) show a number of narrow, well isolated structures which are highly correlated in the different reaction channels (Saini *et al* 1987). Angular momentum measurements indicate groupings of the resonances into sets each with the same spin. The energy spacing between these sets is consistent with that of the rotation of an extremely deformed, rigid, mass 48 system with angular momentum equal to the measured values. Perhaps not coincidentally, the moment of inertia associated with this rotation is also close to that of two deformed ^{24}Mg nuclei touching end-to-end.

The pattern of resonance widths in these heavier systems is, however, quite different from that of the lightest systems. In the case of $^{12}C + {}^{12}C$, for example, as has been discussed, the partial width for decay into the elastic width is both a large fraction of the total resonance width and of the 'single-particle' value—the origin of the name 'nuclear molecule'. For the heavier systems, the elastic channel partial width is typically only of order 1% of the total resonance width and of the 'single-particle' value. It is also true that,

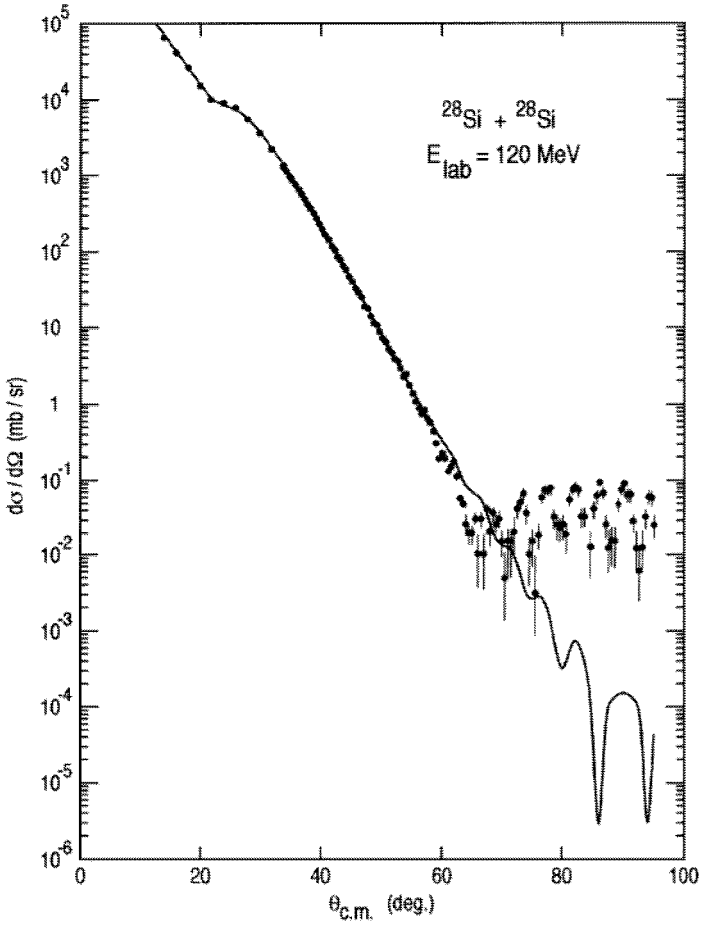

Figure 17. Elastic scattering angular distribution for $^{28}\mathrm{Si} + {}^{28}\mathrm{Si}$ at $E_{\mathrm{LAB}} = 120$ MeV (Betts 1984a). The angular period of the large-angle oscillations corresponds to $|P_{40}(\cos\theta)|^2$.

whereas for the lightest systems the total width of the resonances can be accounted for in experimentally measured channels, for the heavier systems only approximately one-third of the total width is observed in binary reaction channels. These two features speak for a more complex underlying structure for these resonances than the simple molecule of the light systems. Nevertheless, the resonances in $^{28}\mathrm{Si} + {}^{28}\mathrm{Si}$ and $^{24}\mathrm{Mg} + {}^{24}\mathrm{Mg}$ scattering have much larger overlap with a simple molecular configuration than the 'normal' states in the respective nuclei at the same excitation energy and spin. Finally, we note that searches (Betts 1984a) for similar narrow resonances in even heavier systems, such as $^{40}\mathrm{Ca} + {}^{40}\mathrm{Ca}$, have so far proved negative.

2.8. Recent advances—break-up studies and multiparticle decays

Recently, a number of new experimental methods have been applied to the problem of nuclear molecules. These new techniques represent an approach to studying these highly clustered states in light nuclei which is complementary to that used in the examination of heavy-ion scattering resonances as described above. In addition, very recent developments in

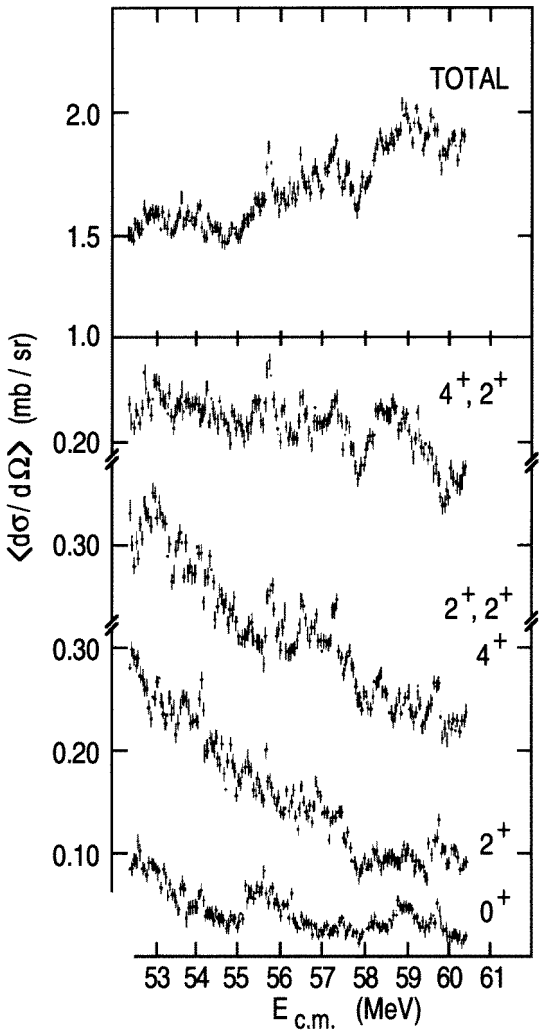

Figure 18. Angle-averaged excitation functions for elastic and inelastic scattering of ^{28}Si + ^{28}Si (Betts *et al* 1981).

detector technology have allowed the study of reactions which were previously inaccessible to experiment. Such techniques may have yielded evidence for even more unusual nuclear molecular states, and have certainly added to the wealth of data already available on this phenomenon.

2.8.1. Break-up reactions. The motivation for studying break-up reactions involving light nuclei originates from the desire to directly observe the fission-like decay of the quasi-molecular state into its constituent fragments, for example ^{24}Mg into two ^{12}C nuclei. Here, the nucleus of interest is raised to a high excitation energy by some scattering mechanism, and the subsequent fission-like decay is observed by detection of the two decay fragments. One advantage of this approach is that the nature of the reaction yields an enhanced sensitivity to states with quasi-molecular character, which, by definition, have

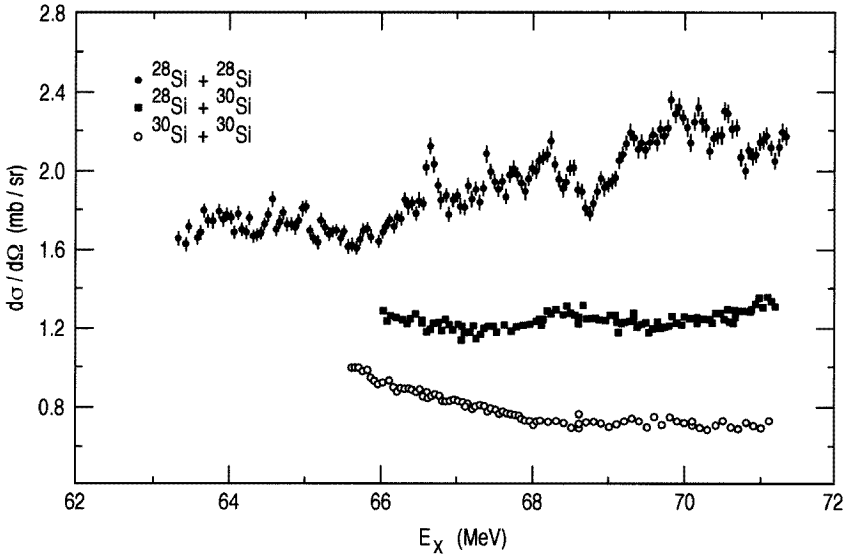

Figure 19. Comparison of excitation functions for large-angle elastic and inelastic scattering of ^{28}Si + ^{28}Si, ^{28}Si + ^{30}Si and ^{30}Si + ^{30}Si (Betts 1984a).

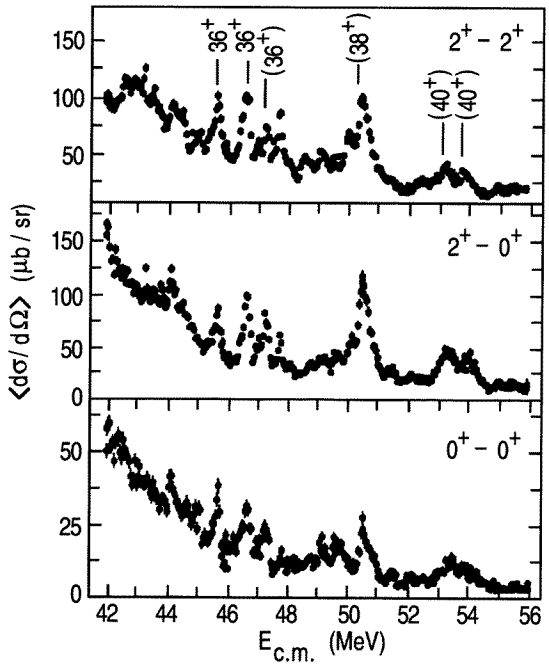

Figure 20. Elastic and inelastic scattering excitation functions for ^{24}Mg + ^{24}Mg (Zurmühle *et al* 1983, Wuosmaa *et al* 1990). The assigned resonance spins are indicated.

large widths for heavy fragment decay. In addition, many of the complications in scattering or transfer reactions are avoided, as the interference between direct potential scattering and resonant amplitudes does not exist in the break-up channel. Finally, a wide range

of excitation energies in the nucleus of interest can be studied in a single experiment, without the need for time-consuming, excitation-function measurements. Limitations to this approach also exist, however. The connection between the states observed in break-up reactions and resonances in scattering reactions is often tenuous. The detection efficiency for break-up reactions is generally small compared to that for scattering reactions, and the break-up reaction mechanism, which can be an important factor in the understanding of the experimental results, is generally not well understood in many cases (Gyapong *et al* 1994).

The first experiments studying the fission-like decay of ^{24}Mg were by electro-fission, i.e. ^{24}Mg(e, e$'^{12}$C)^{12}C. These were performed, first using track detectors (Chung *et al* 1974), and then with conventional detector telescopes (Sandorfi *et al* 1980). Discrete states were identified which decayed into ^{12}C + ^{12}C; however, these were found also to have significant parentage with the ground state of ^{24}Mg, and were therefore believed not to be closely related to quasi-molecular resonances seen in ^{12}C + ^{12}C scattering. The complementary radiative capture reaction ^{12}C(^{12}C, γ)^{24}Mg was examined by Nathan *et al* (1981). A number of resonances between $E_{\rm cm} = 5$ and 9 MeV were identified, and each assigned a spin of 2^+. These were also thought not to be related to the quasi-molecular resonances, but rather to reflect some intermediate configurations which possessed a large ^{12}C + ^{12}C cluster component, and yet were structurally related to the ground state of ^{24}Mg. It was suggested, however, that some influence of the molecular configurations could be present in the data. These data are shown in figure 21.

First attempts to observe quasi-molecular states in ^{24}Mg in fission-like break-up reactions were made by groups at Daresbury and Berkeley (Fulton *et al* 1986, Wilczynski *et al* 1986). In these experiments, ^{24}Mg beams bombarded ^{12}C targets, and position-sensitive, silicon-detector telescopes placed at forward scattering angles were used to detect both ^{12}C fragments from the decay of the excited ^{24}Mg nuclei. The kinematic information was sufficient to reconstruct the momentum of the third unobserved ^{12}C, and hence fully determine the scattering kinematics. Events in which all three ^{12}C nuclei were left in their ground states were isolated by determining the total reaction Q value, $Q_{\rm ggg}$, and for these events, the excitation energy of the decaying ^{24}Mg nucleus was determined. The excitation-energy spectrum for ^{24}Mg$^* \rightarrow$ ^{12}C + ^{12}C from Fulton (1991) appears in figure 22. Evidence for states at excitation energies between 20 and 25 MeV was found, and in one case the angular correlations of the ^{12}C decay fragments suggested a spin for the state at $E_{\rm x} = 21.9$ MeV of 2^+. It was suggested that these states could correspond to those populated as resonances in ^{12}C + ^{12}C scattering. Later measurements with improved excitation-energy resolution identified more structure, and improved angular correlation data permitted the assignment of spins for several of the states identified (Fulton *et al* 1994). The sequence of angular momenta thus determined resembled a rotational sequence for an object with a moment of inertia consistent with that of a strongly-deformed quasi-molecular configuration.

Subsequent measurements of the ^{12}C(^{20}Ne,^{12} C^{12}C)^{8}Be reaction revealed similar features in the same range of excitation energies in ^{24}Mg as were observed in the ^{24}Mg + ^{12}C break-up measurements (Fulton *et al* 1994). While spin assignments could not be obtained for the states populated in this transfer reaction, the correspondence in energy between the states populated in ^{24}Mg break-up and those in the ^{8}Be transfer was highly suggestive that indeed the same levels were being populated. These results indicated that the states being observed might be associated with a molecular α–^{16}O–α configuration which had been previously suggested to account for resonances in the barrier region in ^{12}C + ^{12}C scattering (Marsh and Rae 1985).

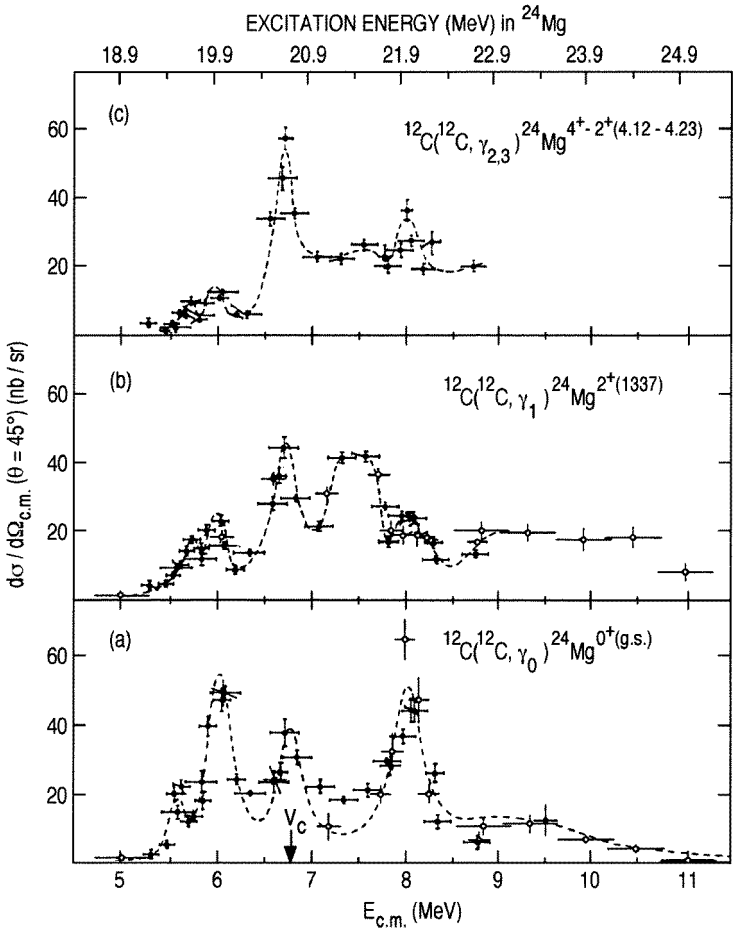

Figure 21. Excitation functions for ^{12}C(^{12}C, γ)^{24}Mg for different final states (Sandorfi and Nathan 1978, Nathan *et al* 1981).

The idea that more exotic nuclear-molecular configurations could exist in light alpha-particle nuclei parallels the first observation of the $^{12}C + {}^{12}C$ scattering resonances. In 1966, Morinaga (Morinaga 1966) considered the systematics of the then known levels in 4n conjugate nuclei and suggested that many properties of the spectra of these nuclei could be explained by considering molecule-like configurations built up out of alpha-particle constituents. Subsequent to that, Ikeda *et al* (1968) categorized such configurations in a simple and straightforward way, arranging possible molecular configurations in light 4n nuclei according to their separation energy. Their prediction was that, for example, in ^{24}Mg where the threshold for decay into $^{12}C + {}^{12}C$ is 13.9 MeV, it is in this region and above that states in ^{24}Mg with this molecular character might be observed. The Ikeda picture also contained a variety of more complicated molecular shapes, consisting of combinations of alpha particles, ^{12}C and ^{16}O clusters. Only a few such configurations were thought to have been observed, however, as many of the decays of such structures would lead to final states which contained many particles, and which were quite difficult to study experimentally.

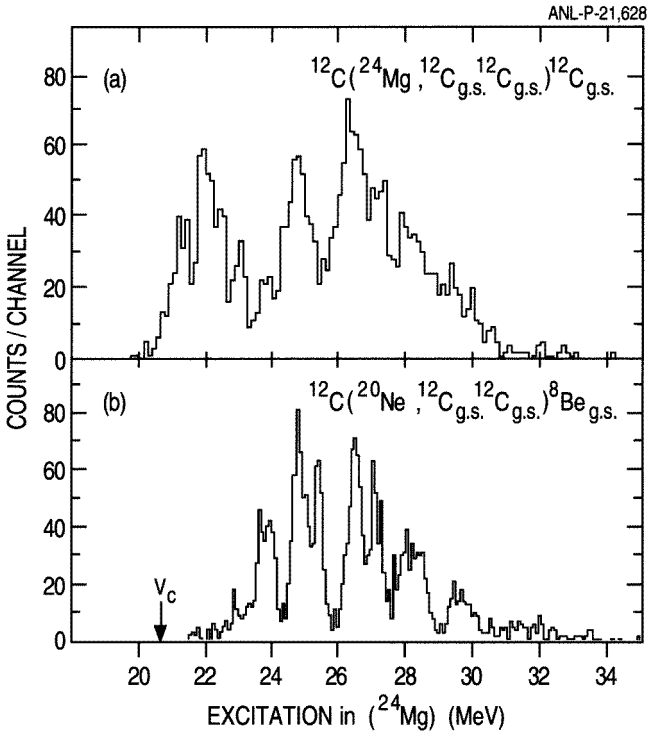

Figure 22. (a) Excitation energy spectrum of ^{24}Mg in the reaction ^{12}C(^{24}Mg,^{12}C^{12}C)^{12}C at 170 MeV. (b) From the reaction ^{12}C(^{20}Ne,^{12}C^{12}C)^{8}Be at 180 MeV (Fulton *et al* 1991, 1994).

An early example of an experiment designed to identify an extended alpha-particle cluster molecule was carried out by Chevallier *et al* (1967), who studied the $\alpha + {}^{12}\mathrm{C} \rightarrow {}^{8}\mathrm{Be} + {}^{8}\mathrm{Be}$ reaction. The two alpha particles from the decay of one of the unbound ^{8}Be nuclei were detected in silicon surface barrier detectors and only events where the alpha-particle energies were consistent with a ^{8}Be decay were kept. Chevallier *et al* identified a series of resonances in this transfer reaction whose spin sequence was consistent with that of a rotational band built on a highly-deformed structure resembling a chain or line of four alpha particles.

The Morinaga/Ikeda picture predicted similarly deformed states in heavier nuclei. Several other rather different calculations of the structure of 4n conjugate nuclei heavier than ^{16}O also predicted similar configurations, and one particularly interesting case was ^{24}Mg. In this nucleus, cluster calculations as well as deformed shell models suggested that these extremely deformed objects may exist at high excitation energy in the spectrum of excited states in ^{24}Mg. It was also predicted that such a structure might decay into lighter fragments with similar molecular character. For example, the excited 0_2^+ state in ^{12}C at 7.65 MeV has been suggested to possess deformed alpha cluster structure (Takigawa and Arima 1971), and extended alpha-chain-like molecules in ^{24}Mg might therefore decay into two deformed $^{12}\mathrm{C}(0_2^+)$ clusters.

With the recent availability of finely-segmented silicon strip detectors, the simultaneous detection of the six alpha particles from the decay of the two ^{12}C nuclei in the $^{12}\mathrm{C}(0_2^+) + {}^{12}\mathrm{C}(0_2^+)$ final state became possible. This reaction was of interest not only from the structural perspective, but also from the reaction-model standpoint, as this channel is mismatched by

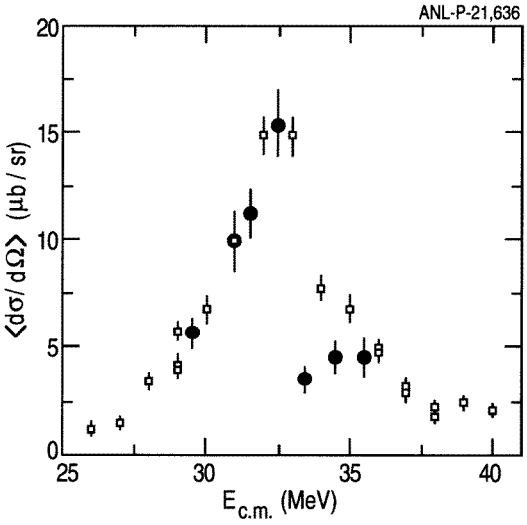

Figure 23. Excitation function for the $^{12}C(^{12}C,^{12}C(0_2^+))^{12}C(0_2^+)$ reaction (Wuosmaa *et al* 1992, 1994a).

six or more units of angular momentum. Due to this large angular momentum mismatch, an explanation of any kind of resonance-like features in this channel as due to direct reactions would be precluded. One measurement identified a broad structure in the excitation function for this channel, which is shown in figure 23 (Wuosmaa *et al* 1992). The large width implied that if a resonant mechanism was at work, the structure likely reflected the contributions of many overlapping partial waves. This conclusion was borne out by angular distribution data (figure 24), which indicated that while the data were predominantly characterized by dominant angular momenta near 14–16$\hbar$ the effects of many other partial waves were evident (Wuosmaa 1994). Rae *et al* (1992) interpreted this result as possible evidence for a structure formed by an almost degenerate set of overlapping rotational states called a 'shape eigenstate'. The calculated angular distribution expected from this model is shown as the full curve in figure 24.

These results were also compared to the cluster model results of Marsh and Rae 1985), and it was noted that the energy and angular momenta reflected by the data lay very close to the expected crossing point of rotational bands built on molecular cluster configurations which resembled ^{12}C(g.s.) clusters, and a linear six-alpha-particle configuration, respectively. One possible interpretation is that this excitation-function feature then reflects an interplay between the nuclear structures of the colliding nuclei and the compound system, and the dynamic properties of the scattering reaction, as suggested by some recent calculations by Hirabayashi *et al* (1995). Clearly, however, the techniques that were used open up many other avenues for the study of complex reactions and final states previously inaccessible to experiment.

3. Theory of nuclear molecules

3.1. Early ideas

As we have mentioned in the introduction to this review, the very first experimental papers of Bromley and collaborators already contained the suggestion that the observed resonances

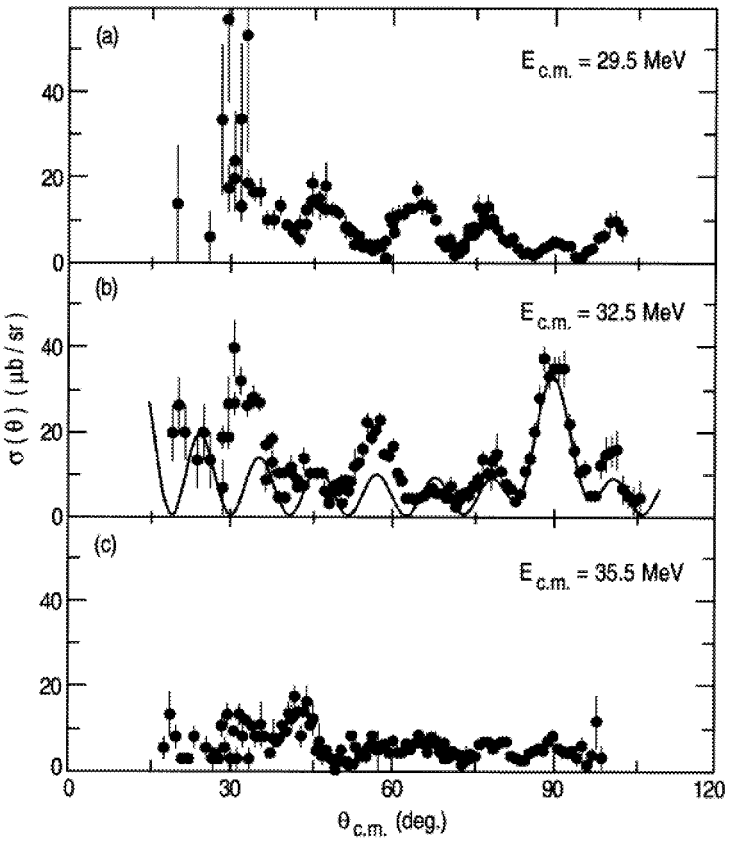

Figure 24. Angular distribution data for the $^{12}C(^{12}C, ^{12}C(0_2^+))^{12}C(0_2^+)$ reaction (Wuosmaa *et al* 1994a). The full curve in (b) is from Rae *et al* (1992).

in $^{12}C + ^{12}C$ scattering and reactions might correspond to a molecule-like configuration of the two ^{12}C nuclei stabilized by the existence of a pocket at large distance in the potential describing their relative motion. The possible origins of this pocket were discussed shortly thereafter in papers by Vogt and McManus (1960) and Davis (1960). In the first of these, the effects of deformation of the ^{12}C nuclei in producing such a pocket was discussed and the narrow resonances interpreted as the spectrum of vibrational and rotational excitations in this potential. Davis (1960) used a phenomenological potential derived from optical model analyses of $^{12}C + ^{12}C$ elastic scattering and demonstrated the existence of quasi-bound states in the pocket formed in the total potential consisting of nuclear, Coulomb and centrifugal components as shown in figure 25. In all this work, it was recognized that the fundamental challenges for any theoretical description were to account for the narrow width of the resonances and the remarkable contrast in the complexity of the resonance spectrum between (at that time only) $^{12}C + ^{12}C$ and $^{16}O + ^{16}O$. Any successful model must, therefore, include sufficient nuclear structure effects to produce differences between adjacent systems and yet provide a weak enough coupling between the resonance and compound nuclear states so as to maintain the narrow widths.

Somewhat later, prompted by observations of $^{12}C + ^{12}C$ resonances at even lower energies than the original Chalk River measurements, it was suggested by Michaud and

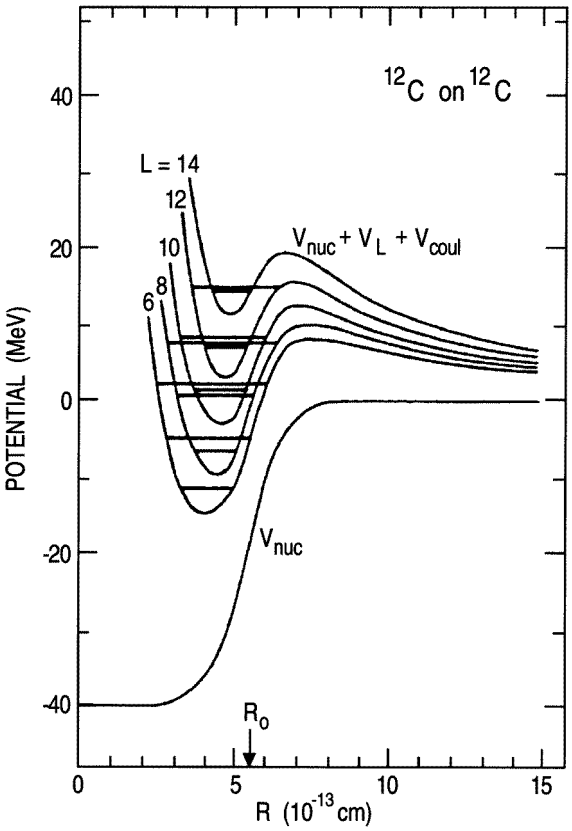

Figure 25. Potential from Davis (1960) used to predict the locations of quasi-bound states in the $^{12}C + {}^{12}C$ interaction.

Vogt (1969, 1972) that an appropriate model description could be obtained if the scattered nuclei were described in the alpha cluster model. In this way, it was possible to introduce the additional degrees of freedom necessary to reproduce the complexity of the molecular spectrum without the enormous increase in the number of states that comes from inclusion of all the degrees of freedom of the individual nucleons. In this way a set of states (doorways), intermediate in complexity between the entrance channel and the compound nucleus, was produced. This approach also provided a connection to the original ideas of extended alpha-particle cluster configurations in light nuclei (Morinaga 1966, Ikeda *et al* 1968). Detailed calculations were, however, beyond the scope of available resources at that time.

A particularly important alternative idea was due to Nogami and Imanishi (Imanishi 1968) who modified the simple potential scattering picture of Davis (1960) by inclusion of inelastic scattering of one of the ^{12}C nuclei to its first excited $J^\pi = 2^+$ state. The coupling of this degree of freedom to the pure potential resonances in a coupled channel treatment was then able to account for many of the observed features of the data.

With some exceptions, the progress of theoretical understanding has always been closely related to these basic ideas.

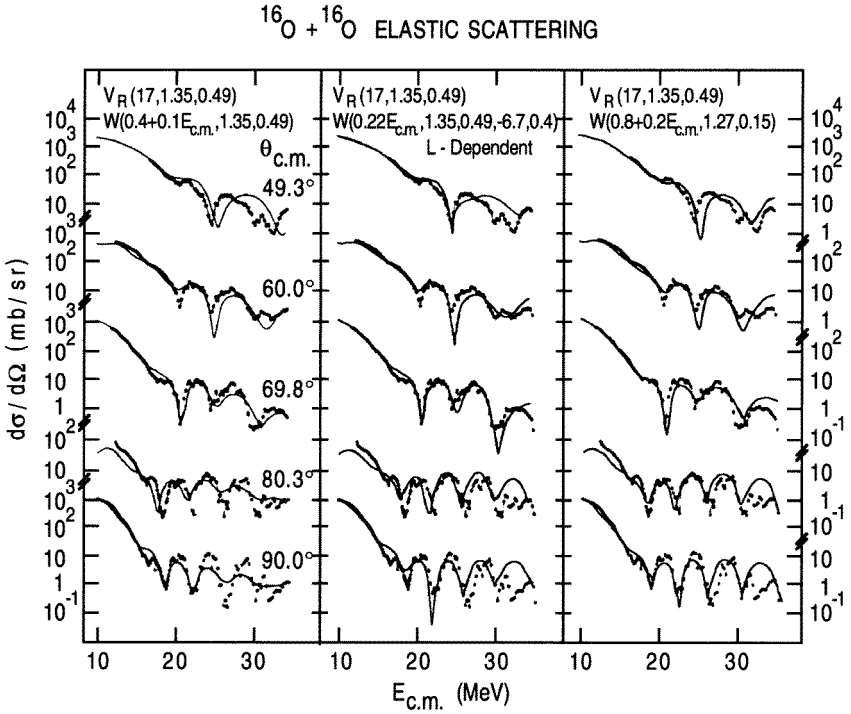

Figure 26. Optical model fits to $^{16}O + {}^{16}O$ elastic scattering data (Gobbi *et al* (1973).

3.2. Potential scattering

Following the initial suggestions of Davis (1960) and Vogt and McManus (1960), considerable effort went into attempts to describe the energy-dependent structures in elastic scattering as resonances in the scattering potential. As shown in figure 25, quasi-bound states may exist in the pocket formed by the sum of the nuclear, Coulomb and centrifugal components of the ion–ion potential. The choice of nuclear potential may be purely phenomenological as in the optical model in which the radial form of the potential is simply parametrized, for example, as a Woods–Saxon form

$$V_{\mathrm{REAL}}(r) = -V_0\{1 + \exp(r - R_{\mathrm{R}})/a_{\mathrm{R}}\}$$
$$W_{\mathrm{IMAG}}(r) = -W_0\{1 + \exp(r - R_{\mathrm{I}})/a_{\mathrm{I}}\}$$

with real and imaginary components with strength V_{REAL} and W_{IMAG}, and radius and diffuseness parameters R and a. Alternatively, more microscopically-based models, such as the folding model and potentials calculated from the two-centre shell models, have also been used to describe the data.

Examples of optical model fits (Gobbi *et al* 1973) to elastic scattering data for $^{16}O + {}^{16}O$ are shown in figure 26 showing that quite equivalent descriptions can be obtained using somewhat different values for the parameters of the imaginary potential. A common feature of all these potentials and those used to describe wide structures in other scattering systems is a strong enough nuclear attraction to produce a pocket in the total potential and an absorption which is weak in the region of this pocket so as to keep the quasi-bound states narrow.

Although potential scattering models have been quite successful in accounting for the overall features of resonances in heavy-ion scattering, it is clear that they fail completely to account for the many narrow structures which are observed. This is perhaps only to be expected as the broad structures correspond to the 'single-particle' molecular resonances of which the narrow resonances are just fragments. Thus, additional degrees of freedom must be added to the simple potential scattering picture.

3.3. Coupled channel models

3.3.1. The Imanishi and the double resonance models. One of the first models which attempted to describe molecular resonances by incorporating coupling between the internal degrees of freedom of the colliding nuclei, and their relative motion, was the double resonance model of Imanishi (1968, 1969). Building on a suggestion by Nogami, Imanishi suggested a mechanism by which a virtual excitation of one of the colliding ^{12}C nuclei to its first excited 2^+ state introduces a sudden change in the molecular potential. The energy transferred from relative motion between the two ions to excitation of one of them causes the system to drop into a bound or quasi-bound state in the new potential. Should the new relative energy of the system coincide with the eigenenergy of one of the quasi-bound molecular states within the potential, a resonance condition would exist.

This model was successful in addressing some of the deficiencies in the simpler potential scattering models. It produced a more complicated spectrum of resonances, with predictions for resonance spins which could be tested by experiment. Imanishi was also able to calculate total widths, and partial widths for decay to $^{12}\mathrm{C}+{}^{12}\mathrm{C}$, and found that these were comparable to the experimental values. The large ^{12}C widths in particular fit in well with the molecular picture of these resonances.

This approach was extended by the Frankfurt theory group, and applied to the $^{16}\mathrm{O}+{}^{16}\mathrm{O}$ (Scheid *et al* 1970) and $^{12}\mathrm{C}+{}^{12}\mathrm{C}$ (Fink *et al* 1972) systems. In each case the idea was the same as Imanishi's, however the number of channels included in the coupling picture was increased. This point became particularly important as data became available at higher and higher energies, where the excitation of more levels in the colliding nuclei could be achieved. The average ion–ion optical potentials used were obtained by comparison to gross structure in the elastic scattering channels, and were based on a Thomas–Fermi model of the nucleus. For the $^{16}\mathrm{O}+{}^{16}\mathrm{O}$ case, the resulting ion–ion potentials had real quasi-bound states up to $L = 10$; the potentials for higher partial waves could only support virtual resonances. In their picture, a partial wave resonates with one of the virtual states in the entrance channel potential, and then by a coupling mechanism one or both of the colliding ions are excited. The crucial point is that in cases where the difference between the incident energy and the excitation energy of one of the different coupling channels matches an eigenenergy of the potential obtained by removing the angular momentum and energy from relative motion, a resonance in the changed potential may be excited. Not surprisingly, as more channels are allowed to participate, the behaviour of the scattering cross section becomes more complicated. Examples of these results appear in figure 27.

These ideas were extended by Kondo *et al* (1978) who performed a comprehensive calculation for the $^{12}\mathrm{C}+{}^{12}\mathrm{C}$ system, where many different possible excitations of the colliding ions were included. In this calculation, Kondo *et al* first identified the likely position of a 2^+ potential scattering resonance near the Coulomb barrier, and then introduced different configurations of the intrinsic excited nuclear molecule. The results were qualitatively in rather good agreement with the observed structures, with a calculated excitation function containing several resonance peaks between centre-of-mass energies of

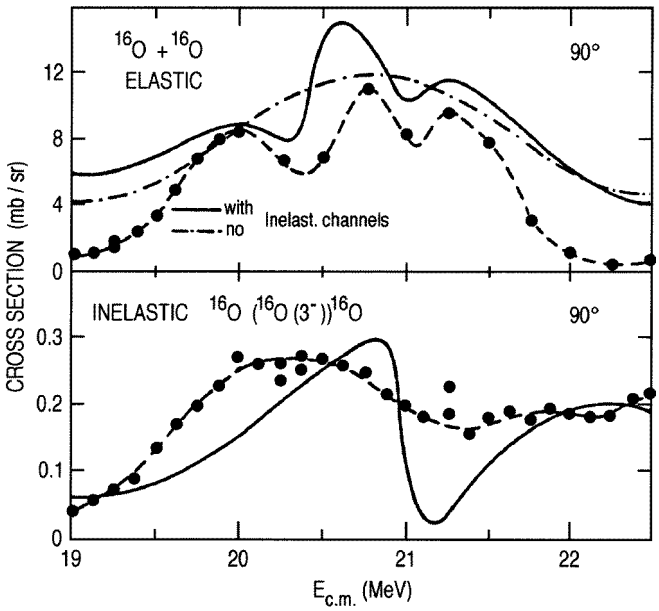

Figure 27. Calculated $^{16}O + {}^{16}O$, $\theta_{cm} = 90^\circ$ excitation curves from Scheid *et al* (1970) for (a) elastic scattering and (b) inelastic scattering to the 3^- (6.13 MeV) state. The data points are from Siemssen *et al* (1967) and Maher *et al* (1969).

4 and 7 MeV, with a spacing on the order of 300 keV, and with total widths near 100 keV (figure 28). Moreover, the calculated ^{12}C reduced widths were again comparable to those obtained from experiment. An important aspect of the calculations was that the model used a scattering potential with rather weak absorption which led to the narrow widths of the calculated resonances. The results obtained using the Imanishi mechanism therefore substantially addressed many of the problems of the early potential scattering pictures.

One criticism of many of these calculations was that, while able to qualitatively reproduce many of the observed features of the scattering excitation functions, the different formulations of the double-resonance picture lacked predictive power. An attempt was made by Matsuse *et al* (1978a, b) to rationalize the problem, and to gain a simpler, physically intuitive model which could be used to predict where the strongest resonance behaviour might be observed. The result was the band crossing model (BCM) which attempted to systematize the occurrence of resonances in heavy-ion scattering. The BCM was applied mainly to resonances observed in inelastic scattering channels, and relied upon angular momentum matching conditions to be satisfied between the elastic and various inelastic scattering channels. In the BCM, a set of rotational states are hypothesized to exist in the elastic scattering channel as well as in various inelastic scattering channels. If the channel spin is non-zero, several quasi-rotational bands will exist in the inelastic scattering channels due to coupling between the orbital angular momentum and the channel spin. For the case in which classically the channel spin and orbital angular momentum are aligned ($J = L + S$), the quasi-rotational trajectory intercepts the elastic band at a particular value of the angular momentum and centre-of-mass energy. In the region of this intersection, it is expected that the coupling strength between the elastic and inelastic channel should be large. In this region of strong coupling, resonance behaviour is expected to be enhanced.

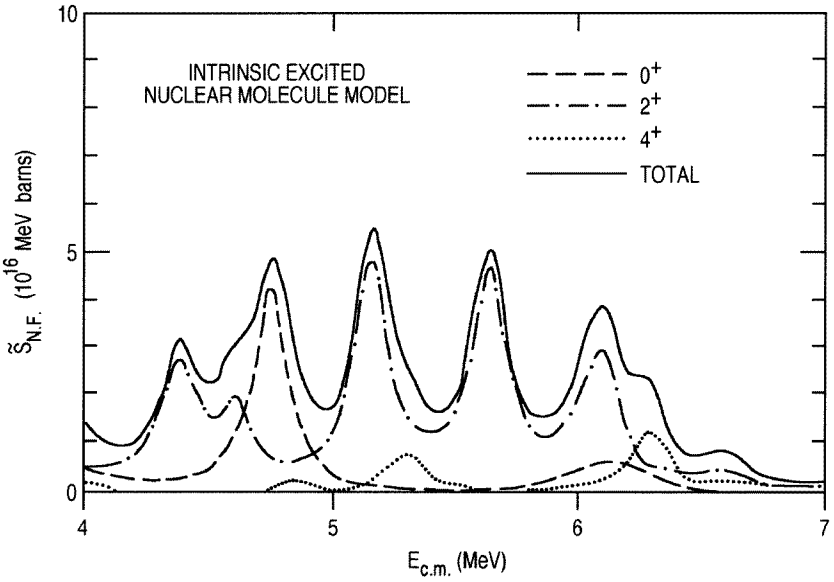

Figure 28. Calculated energy dependence of the nuclear structure factor ($\tilde{S}$), from Kondo *et al* (1978).

A full coupled-channels formulation of the BCM was applied to scattering of $^{12}C + {}^{16}O$ (Matsuse *et al* 1978a), $^{12}C + {}^{12}C$ (Abe *et al* 1979, Kondo *et al* 1979) and $^{16}O + {}^{16}O$ (Kondo *et al* 1980). Results for the $^{12}C + {}^{12}C$ and $^{16}O + {}^{16}O$ systems appear in figure 29, with the data of Cormier *et al* 1978) for $^{12}C + {}^{12}C$, and Kolata *et al* (1977) for $^{16}O + {}^{16}O$. In each case, the excitation curves produced from the BCM are in very good qualitative agreement with the data. The calculated dominant angular momenta for the various structures are also shown in figure 29. As noted in section 2.5, resonance spin assignments are more difficult to make for inelastic excitation, however some progress has been made in this direction using correlation techniques. In the $^{12}C + {}^{12}C$ system, particle–γ-ray correlation measurements 4.43 MeV for the 2^+ excitation by Sugiyama *et al* (1985), and particle–particle correlation measurements 9.64 MeV for the 3^- state by Wuosmaa *et al* (1996) suggest resonance spins two units of angular momentum higher than those obtained from the BCM. Still, the simple picture afforded by the BCM gives considerable insight into the general properties of the scattering reaction that can lead to resonance behaviour.

3.4. Shell structure and clusters

The introduction of nuclear structure effects in the theoretical description of nuclear molecules has largely been based on the two and multi-centre shell models. Of these, the coupled-channels approach described in the preceding section represents a special case of the two-centre model in which the physical states of the colliding nuclei, coupled to the relative motion, are used as a basis. In a more general approach, Preuss and Greiner (1970) calculated potentials for $^{12}C + {}^{12}C$ and $^{16}O + {}^{16}O$ using a two-centre harmonic oscillator model with spin–orbit coupling. Single-particle orbitals were calculated as a function of the separation of the two centres. They distinguished between two limiting cases—'fast' in which the frequency of the oscillator potential remains fixed at the value appropriate to the two nuclei at large separations and 'slow' in which the potential is continuously adjusted to

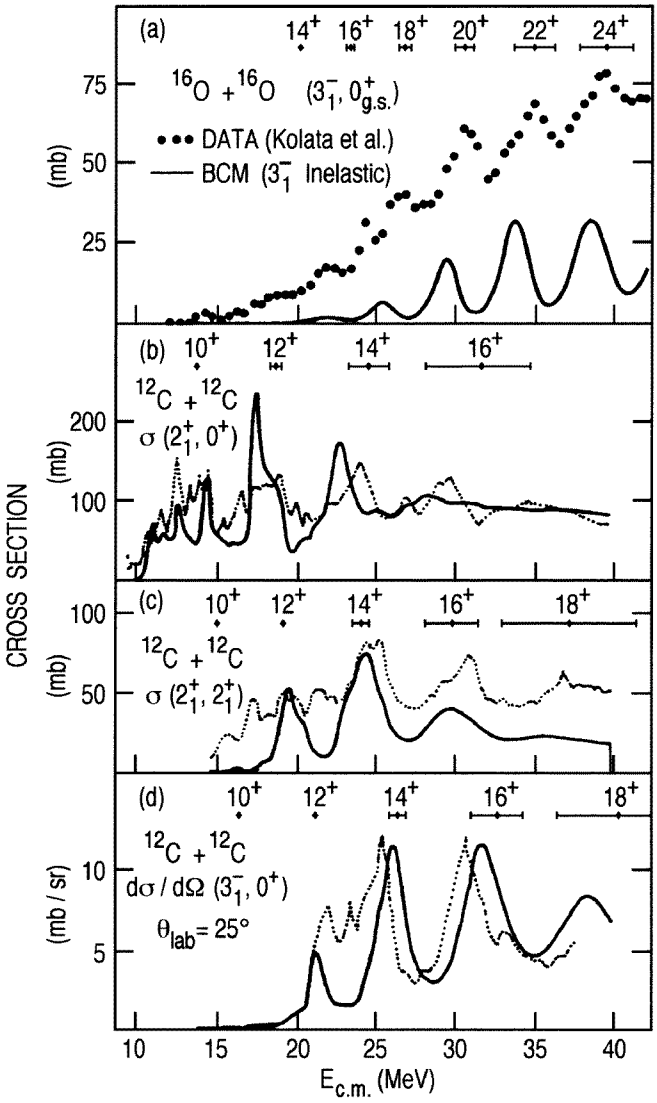

Figure 29. BCM results from Matsuse *et al* (1978a, b), Abe *et al* (1979) and Kondo *et al* (1978, 1979, 1980) plotted with data for inelastic scattering in $^{16}O + {}^{16}O$ and $^{12}C + {}^{12}C$.

conserve the volume of the colliding system. Scattering potentials were calculated from the single-particle energies using the Strutinsky method and the resulting potentials are shown in figure 30. These potentials all show minima at large separations of the colliding nuclei which, in principle, could represent stable molecular configurations.

An interesting, simplified, extension of these ideas was discussed by Harvey 1975) who considered the formation of a composite system from two nuclei with alpha cluster structure described in the harmonic oscillator model with no spin–orbit coupling. As the two nuclei overlap, the constraints applied to the occupancy of the single-particle orbitals by the Pauli principle were followed by the promotion of alpha clusters to unoccupied orbits. The prescription for this promotion was that only the component of the cluster wavefunction

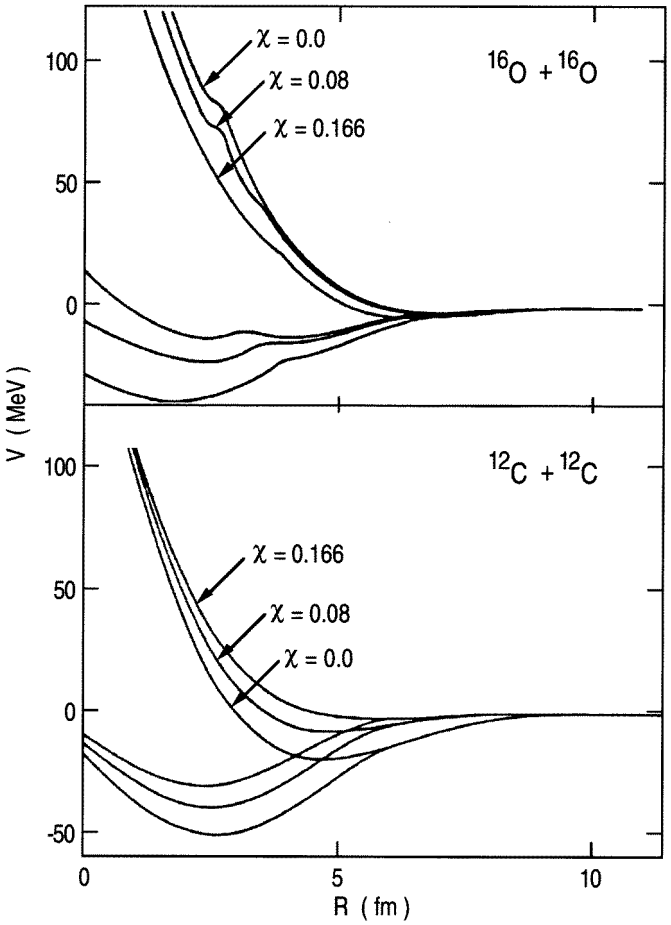

Figure 30. Nuclear potentials for $^{16}O + {}^{16}O$ and $^{12}C + {}^{12}C$ interactions calculated in the framework of the two-centre shell model in the 'fast' and 'slow' approximations (Preuss and Greiner 1970).

along the collision axis was changed, and then only minimally in order to accommodate the Pauli principle. In this way, the cluster wavefunctions of the two separated nuclei could be seen to evolve to specific cluster configurations of the composite system with extremely deformed equilibrium shapes. A set of selection rules for formation and decay of these states into different partitions then followed. A particular result of this simple approach was the realization that, in the case of non-spherical collision systems, quite different sets of states in the composite system would be populated which could naturally explain the striking differences between the ^{12}C (deformed) and ^{16}O (spherical) resonance spectra.

At the same time, Leander and Larsson (1975) published Nilsson–Strutinsky calculations of potential energy surfaces for a number of light nuclei including ^{24}Mg and ^{32}S. These calculations show the potential energy of the nucleus as a function of a number of parameters describing the deformation of the nuclear surface and include a wide range of possible shapes ranging from axially symmetric prolate to flat oblate spheroids—the possibility of non-reflection symmetric shapes was also considered. The result of these calculations for ^{24}Mg is shown in figure 31 which displays contours of equal energy as a function of

the usually defined deformation parameters (ε and γ). Minima which define quasi-stable shapes are shown as shaded. In addition to the moderately deformed ($\varepsilon = 0.45$, $\gamma = 20^\circ$) minimum which corresponds to the ground-state configuration, a number of highly-deformed minima are observed ($\varepsilon = 1.00$, $\varepsilon_3 = 0.30$, $\gamma = 0^\circ$; $\varepsilon = 1.23$, $\gamma = 60^\circ$; $\varepsilon = 1.26$, $\gamma = 42^\circ$ and $\varepsilon = 1.25$, $\gamma = 0^\circ$). It was suggested that these extremely-deformed minima corresponded to shapes with axes in the ratio of simple integers analogous to, the then known, fissioning shape isomers in very heavy nuclei and, subsequently discovered a decade later, superdeformed nuclei. The possible connection to the $^{12}C + {}^{12}C$ molecular resonances was also made at this time (Bromley 1975).

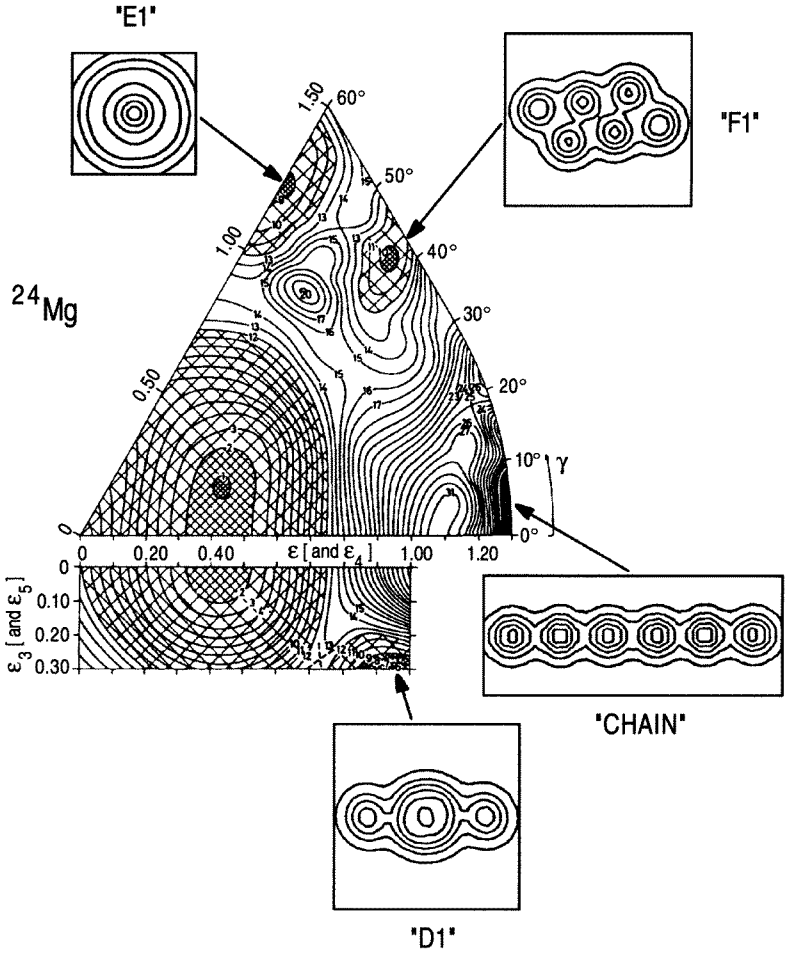

Figure 31. Potential energy surface for ^{24}Mg calculated using the deformed shell model (Leander and Larsson 1975). Associated with the minima in this surface are various quasi-stable cluster configurations (Marsh and Rae 1985).

In parallel with these studies, the original alpha cluster ideas were also developed using models which might be thought of as multi-centre shell models in which each alpha cluster is composed of four nucleus in their own shell model potential centred at the cluster location. Calculations were carried out using this approach for a variety of point symmetries of the constituent clusters (Brink *et al* 1970), Bauhoff *et al* (1980a, b, 1981, 1984) and

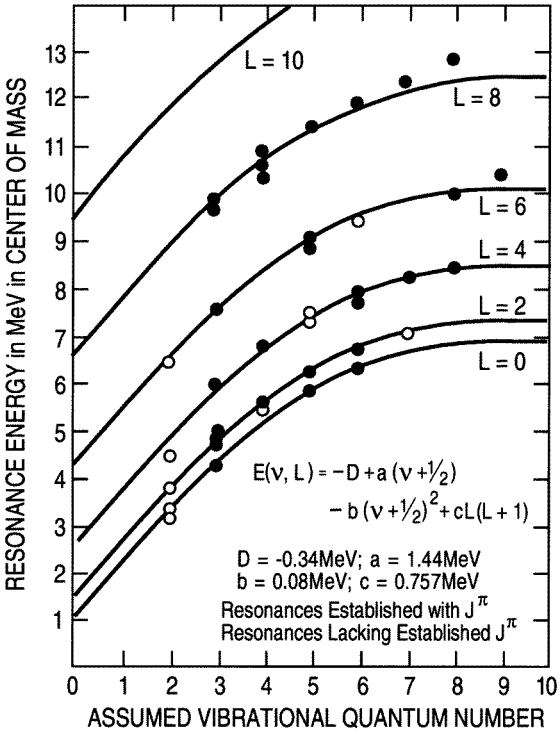

Figure 32. Classification of the low-energy $^{12}C + {}^{12}C$ resonances according to a rotation–vibration scheme (Erb and Bromley 1981, Iachello 1981).

configurations reminiscent of those originally proposed by Morinaga (1966) and Ikeda *et al* (1968) were found to be energetically favoured. Computational limitations, however, restricted the number of configurations which could be studied. The first unconstrained calculation was carried out by Marsh and Rae (1985) who published results for ^{24}Mg which showed a number of quasi-stable configurations of six alpha particles. Strikingly, they were able to associate each of these with the potential energy minima in the Nilsson–Strutinsky calculation of Leander and Larsson as shown in figure 31 in which the calculated densities of the cluster states are associated with the potential energy surface minima. A further interesting aspect of this calculation is the use of the cluster densities to suggest the likely decay modes of each configuration based on the overlaps with specific channels. For example, the configuration 'F1' should predominantly decay to two ^{12}C nuclei in their ground-state configuration (which also includes rotations built on the configuration such as the excited 2^+ state in ^{12}C). Alternatively the configuration 'D1' has large overlap with one ^{12}C in the ground state and the other in the chain-like excited 0^+ state. The use of the selection rules from Harvey's model applied to the dominant oscillator configurations of the deformed minima also gives the same results for the favoured decay modes.

A number of other calculations of potential energy surfaces in the framework of the deformed, rotating shell model have been carried out by the Lund group (Åberg 1991) which show secondary minima at large deformations. For example, the nucleus ^{48}Cr shows a minimum with a 3:1 axis ratio and ^{56}Ni a 2:1 shaped minimum. A particularly interesting feature of these calculations is the weakening and disappearance of the secondary minimum as neutrons are added to ^{56}Ni going to ^{58}Ni and ^{60}Ni. This result is suggestively correlated

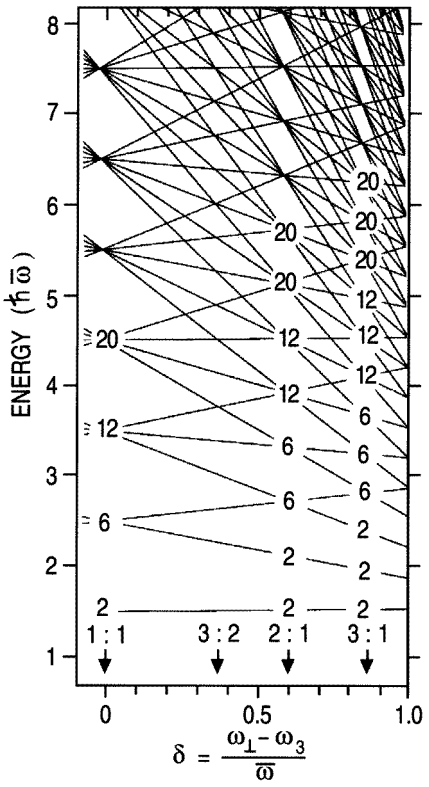

Figure 33. Energy levels of an axially-deformed harmonic oscillator potential in units of $\hbar\bar{\omega} = \hbar(2\omega_\perp + \omega_3)/3$ plotted against deformation $\delta = (\omega_\perp + \omega_3)/\bar{\omega}$. The degeneracies at rational ratios of the frequencies are indicated.

with the disappearance of the narrow resonances in the $^{28}Si + {}^{30}Si$ and $^{30}Si + {}^{30}Si$ systems compared to $^{28}Si + {}^{28}Si$.

Of course the connection of the deformed secondary minima to molecular resonances depends on the relative probability of the decay of states in this minimum, either through the outer barrier to binary nuclear channels or through the inner barrier which represents a mixing of the deformed states with normal compound nuclear states. The competition of these two pathways and with gamma decay between states in the secondary minimum represents a fascinating problem of which nuclear molecules are just one manifestation—the others being 'superdeformed' gamma decaying states and fissioning shape isomers in the heaviest nuclei.

3.5. Symmetries

The most obvious symmetry which appears in the spectra of nuclear molecules is that of rotation. Groupings of resonances with the same spin appear, each separated from each other by energies characteristic of rotation of a di-nuclear molecule-like system. This feature is particularly apparent in the case of the resonance spectrum excited via an entrance channel consisting of identical spin-zero nuclei in which the required Bose symmetry suppresses odd angular momenta. Although this simple spectrum is able to account for the overall

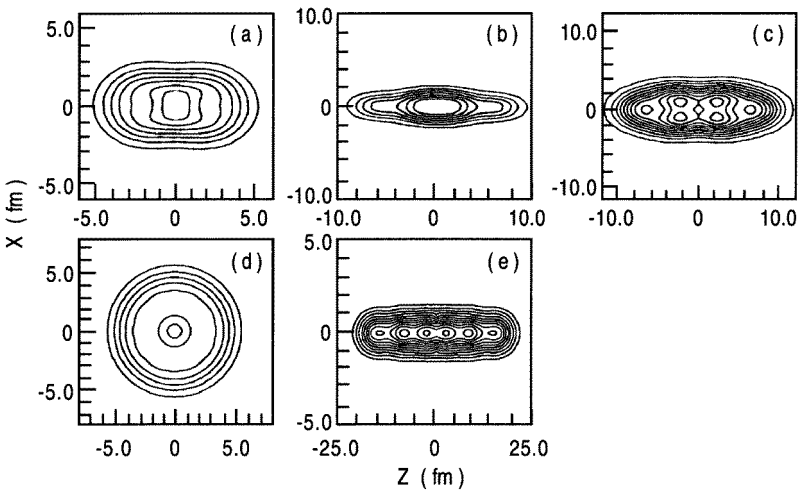

Figure 34. Contours of densities calculated from the harmonic oscillator wavefunctions corresponding to the minima shown in figure 31. Note the correspondence between these shapes and those of the cluster model calculations (Freer *et al* 1995).

features of the resonance spectrum, the presence of numbers of states with the same spin must require additional degrees of freedom.

A number of phenomenologically motivated approaches have been used to try and categorize the experimentally observed spectra, primarily for the $^{12}C + {}^{12}C$ resonances which are the most thoroughly studied. Cindro (1978) applied a rotation–vibration model to the $^{12}C + {}^{12}C$ data and was able to achieve a qualitative agreement with the observed spectrum. More successfully, Iachello (1981) and Erb and Bromley (1981) used quite general considerations to derive an expression for the energy spectrum of a nuclear molecule and obtained impressive agreement with the then available $^{12}C + {}^{12}C$ data as shown in figure 32. More recently, the observation that stability of deformed nuclei occurred when the axes were in the ratio of simple integers (rational) prompted theoretical investigations of the symmetry properties of many-particle states in deformed potentials with rational ratios. The particular potential of interest in this context is the deformed harmonic oscillator which has long been used in nuclear shell model calculations. The first observation is, as shown in figure 33, that whenever the ratios of the oscillator frequencies are rational, large degeneracies occur. These degeneracies give rise to shell gaps which in turn lead to the appearance of secondary minima in the energy surfaces calculated from these single-particle levels for nuclei with the appropriate numbers of nucleons. Further, the spin–isospin degeneracy of the single-particle levels favours alpha-particle clustering in these configurations. The group theoretical properties of such a situation were studied by Rosenthal and Draayer (1989) and further developed by Nazarewicz and Dobaczewski (1992) who showed that these extremely deformed 'magic' nuclei had a unique decomposition into two- or many-centre shell model wavefunctions which indicated a strong connection with the deformed states and molecular configurations as suggested by Marsh and Rae (1985). This connection was underlined by Freer *et al* (1995) who, through calculated density distributions, showed the almost precise correspondence between the deformed shell model and the cluster or many-centre shell models. The densities calculated for the various deformed shell model configurations in ^{24}Mg are shown in figure 34. These are to be compared with the cluster model densities shown in figure 31. Interestingly,

these model wavefunctions exactly follow the Harvey prescription for the evolution of their quantum numbers as a function of radial separation of the clusters. It therefore appears that, underlying the complex spectrum of observed resonances, there may be some quite simple symmetries. The unraveling of this puzzle is for the future.

4. Summary

The vast body of experimental data accumulated over the past three decades has demonstrated very strong indications that nuclear states of molecular nature do in fact exist over a wide range of nuclei. Many of the detailed properties of these resonant states vary from system to system, but the general characteristics are quite similar. The most striking examples have been found in resonance reactions involving scattering of symmetric and near-symmetric, heavy-ion systems. The systematic trends of the spins and the energies of resonances in many systems from $^{4}\mathrm{He} + {}^{4}\mathrm{He}$ to $^{28}\mathrm{Si} + {}^{28}\mathrm{Si}$ follow trends which suggest the formation of highly-deformed systems with molecular character. These suppositions are supported by theoretical expectations. The narrow widths, and the corresponding long lifetimes, of the observed resonances are frequently consistent with that for a system which survives for a few rotations, as expected for a quasi-stable molecular complex. Finally, the reduced decay widths, or the 'single-particle' widths, generally indicate a large overlap of the resonance configuration with that for a molecular single-particle.

Missing, however, in this picture is any single piece of experimental data which possesses direct sensitivity to the shape of the nuclear system. In particular, the observation of direct radiative transitions between members of the observed molecular rotational bands would directly show the structural connection between the two participating states, and the absolute transition rate would directly demonstrate the extended nature of the charge distribution which is implicit in the molecular picture. Such measurements are, however, extremely challenging as the competition between particle decay resonances and their radiative decay results in expected branching ratios for the gamma rays of less than 10^{-5}, even in the most favorable cases. Efforts have been made to measure such transitions, for example by Metag *et al* (1982, 1984), who set upper limits on the gamma decay branch which were somewhat smaller than those expected for a quasi-molecular gamma ray transition, possibly calling into question the quasi-molecular interpretation of some of the resonances in $^{12}\mathrm{C} + {}^{12}\mathrm{C}$ scattering. Since these measurements were made, however, there has been enormous progress in experimental techniques which suggests that it may be timely to revisit these questions. Perhaps more sophisticated experiments are now in order using, for example, one of the new generation of high-resolution 4-π intrinsic Ge detector arrays coupled with a state-of-the-art particle detection system.

Theoretically, the situation is similar. The coupled-channels reaction framework which has evolved over the years has been able to qualitatively, and in some cases quantitatively, explain many of the observed features of heavy-ion resonances, including energy-spin systematics, partial and total decay widths. Many of these models, however, lack a connection to the microscopic properties of the nuclear system. From another viewpoint, nuclear structure or cluster models also point to the existence of molecule-like configurations at extreme conditions of excitation energy or angular momentum, but these models are currently unable to make any prediction as to what might be observed in a real heavy-ion reaction. Some advances in this direction might be made by combining a coupled-channels description of the scattering process with microscopically derived molecular configurations, or perhaps the calculation of fission decay widths within the framework of the cranked shell model, or from the time-dependent Hartree–Fock formalism.

Acknowledgment

This work was supported by the US Department of Energy, Nuclear Physics Division.

References

Abe Y *et al* 1979 *Phys. Rev.* C **19** 1365–71
Åberg S 1991 *Proc. Workshop on the Interface Between Nuclear Structure and Heavy-Ion Reaction Dynamics (University Notre Dame, IN, 1990)* ed R R Betts and J J Kolata (Bristol: IOP) pp 143–62
Almqvist E *et al* 1960 *Phys. Rev. Lett.* **4** 515–17
——1963 *Phys. Rev.* C **130** 1140–52
Andritsopoulos G *et al* 1980 *Phys. Rev.* C **21** 1648–51
Barrette J *et al* 1978 *Phys. Rev. Lett.* **40** 445–8
Basrak Z *et al* 1976 *Phys. Lett.* **65B** 119–21
Bauhoff W, Schultheis H and Schultheis R 1980a *Phys. Lett.* **95B** 5–8
——1980b *Phys. Rev.* C **22** 861–8
——1981 *Phys. Lett.* **106B** 278–80
——1984 *Phys. Rev.* C **29** 1046–55
Beene J R *et al* 1980 *Phys. Rev.* C **21** 167–74
Betts R R 1984a *Proc. Conf. on Nuclear Physics with Heavy Ions (Stony Brook, NY, 1983)* ed P Braun Münzinger (New York: Harwood) pp 347–67
——1984b *Proc. 4th Int. Conf. on Clustering Aspects of Nuclear Structure (Chester, 1984)* ed J S Lilley and M A Nagarajan (Dordrecht: Riedel) pp 133–51
Betts R R *et al* 1979 *Phys. Rev. Lett.* **43** 253–6
——1981a *Phys. Lett.* **100B** 117–20
——1981b *Phys. Rev. Lett.* **47** 23–6
Braun-Münzinger P *et al* 1977 *Phys. Rev. Lett.* **38** 944–7
Brink D M *et al* 1970 *Phys. Lett.* **33B** 143–6
Bromley D A 1975 *Proc. 2nd Int. Conf. Clustering Phenomena in Nuclei (College Park, MD), USERDA Report* ORO-4856-26, pp 465–95
Bromley D A *et al* 1960 *Phys. Rev. Lett.* **4** 365–7
——1961 *Phys. Rev.* **123** 878–93
Cannell L E *et al* 1979 *Phys. Rev. Lett.* **43** 837–40
Chevallier P *et al* 1967 *Phys. Rev.* **160** 827–34
Chung A H *et al* 1974 *Phys. Lett.* **53B** 244–6
Cindro N 1978 *J. Phys. G: Nucl. Phys.* **4** L23–7
Clover M R *et al* 1978 *Phys. Rev. Lett.* **40** 1008–10
Cormier T M *et al* 1977 *Phys. Rev. Lett.* **38** 940–3
——1978 *Phys. Rev. Lett.* **40** 924–7
Davis R H 1960 *Phys. Rev. Lett.* **4** 521–2
Erb K A and Bromley D A 1981 *Phys. Rev.* C **23** 2781–4
——1985 *Treatise on Heavy-Ion Science* vol 3, ed D A Bromley (New York: Plenum) pp 201–310
Erb K A *et al* 1976 *Phys. Rev. Lett.* **37** 670–3
——1980 *Phys. Rev.* C **22** 507–14
Ferguson A J 1965 *Angular Correlation Methods in Gamma-Ray Spectroscopy* (Amsterdam: North-Holland)
Fink H-J *et al* 1972 *Nucl. Phys.* A **188** 259–88
Freer M F, Betts R R and Wuosmaa A H 1995 *Nucl. Phys.* A **587** 36–54
Freer M and Merchant A C 1997 *J. Phys. G: Nucl. Part. Phys.* **23** 261–323
Fulton B R and Rae W D M 1990 *J. Phys. G: Nucl. Part. Phys.* **16** 333–64
Fulton B R *et al* 1986 *Phys. Lett.* **181B** 233–7
——1991 *Phys. Lett.* **267B** 325–9
——1994 *J. Phys. G: Nucl. Part. Phys.* **20** 151–7
Galster W *et al* 1977 *Phys. Rev.* C **15** 950–3
Gobbi A *et al* 1973 *Phys. Rev.* C **7** 30–43
Greiner W, Park J Y and Scheid W 1995 *Nuclear Molecules* (Singapore: World Scientific)
Gyapong G J *et al* 1994 *Nucl. Phys.* A **579** 207–24
Halbert M L *et al* 1974 *Phys. Lett.* **51B** 341–4

Harvey M 1975 *Proc. 2nd Int. Conf. on Clustering Phenomena in Nuclei (College Park, MD), USERDA Report* ORO-4856-26, pp 549–64
Hirabayashi Y, Sakuragi Y and Abe Y 1995 *Phys. Rev. Lett.* **74** 4141–4
Hurd J R *et al* 1980 *Phys. Rev.* C **22** 528–39
Iachello F 1981 *Phys. Rev.* C **23** 2778–80
Ikeda K, Takigawa N and Horiuchi H 1968 *Prog. Theor. Phys. Suppl.* Extra Number 464–75
Imanishi B 1968 *Phys. Lett.* **27B** 267–70
——1969 *Nucl. Phys.* A **125** 33–56
Jääskeläinen M 1983 *Nucl. Instrum. Methods* **204** 385–405
Jachcinski C M *et al* 1979 *Phys. Lett.* **87B** 354–8
Kettner K-U *et al* 1977 *Phys. Rev. Lett.* **38** 337–40
Kolata J J *et al* 1977 *Phys. Rev.* C **16** 891–4
Kondo Y *et al* 1978 *Prog. Theor. Phys.* **59** 465–79
——1979 *Phys. Rev.* C **19** 1356–65
——1980 *Phys. Rev.* C **22** 1068–79
Konnerth *et al* 1985 *Phys. Rev. Lett.* **55** 588–91
Korotky S K *et al* 1979 *Phys. Rev.* C **20** 1014–20
Kovar D *et al* 1979 *Phys. Rev.* C **20** 1305–31
Kubono S *et al* 1979a *Phys. Lett.* **84B** 408–10
——1979b *Phys. Lett.* **81B** 140–2
Kutt P H *et al* 1985 *Phys. Lett.* **155B** 27–30
Kyoto 1988 *Proc. 5th Int. Conf. on Clustering Aspects in Nuclear and Subnuclear Systems (Kyoto, 1988), J. Phys. Soc. Japan Suppl.* **58** 1989
Leander G and Larsson S E 1975 *Nucl. Phys.* A **239** 93–113
Maher J V *et al* 1969 *Phys. Rev.* **188** 1665–82
Malmin R E *et al* 1972 *Phys. Rev. Lett.* **28** 1590–3
Marsh S and Rae W D M 1985 *Phys. Lett.* **180B** 185
Matsuse T *et al* 1978a *Prog. Theor. Phys.* **59** 1009–11
——1978b *Prog. Theor. Phys.* **59** 1904–21
Metag V *et al* 1982 *Phys. Rev.* C **25** 1486–93
——1984 *Proc. Conf. on Nuclear Physics with Heavy Ions (Stony Brook, NY, 1983)* ed P Braun Münzinger (New York: Harwood) pp 391–401
Michaud G and Vogt E W 1969 *Phys. Lett.* **30B** 85–7
——1972 *Phys. Rev.* C **5** 350–68
Morinaga H 1966 *Phys. Lett.* **21** 78–9
Nathan A M *et al* 1981 *Phys. Rev.* C **24** 932–43
Nazarewicz W and Dobaczewski J 1992 *Phys. Rev. Lett.* **68** 154–7
Pate S F *et al* 1990 *Phys. Rev.* C **41** R1344–7
Paul M *et al* 1978 *Phys. Rev. Lett.* **40** 1310–2
Preuss K and Greiner W 1970 *Phys. Lett.* **33B** 197–202
Rae W D M, Merchant A C and Buck B 1992 *Phys. Rev. Lett.* **69** 3709–12
Rae W D M *et al* 1987a *Phys. Lett.* **184B** 133–8
——1987b *Phys. Lett.* **198B** 49–52
Reilly W *et al* 1973 *Nuovo Cimento* **13** 913–21
Rosenthal G and Draayer J P 1989 *J. Phys. A: Math. Gen.* **22** 1323–7
Rybiki F, Tamura T and Satchler G R 1970 *Nucl. Phys.* A **146** 659–76
Saini S and Betts R R 1984 *Phys. Rev.* C **29** 1769–76
Saini S *et al* 1987 *Phys. Lett.* **185B** 316–20
Sanders S J *et al* 1980 *Phys. Rev.* C **21** 1810–8
Sandorfi A M and Nathan A M 1978 *Phys. Rev. Lett.* **40** 1252–5
Sandorfi A M *et al* 1980 *Phys. Rev. Lett.* **45** 1615–8
Santorini 1994 *Proc. 2nd Int. Conf. on Clustering Phenomena in Nuclear and Atomic Systems (Santorini, 1993) Z. Phys.* A **349** 195–370
Satchler G R 1983 *International Monographs in Physics* (New York: Oxford University Press) pp 165–78
Scheid W *et al* 1970 *Phys. Rev. Lett.* **25** 176–80
Shapira D *et al* 1979 *Phys. Rev. Lett.* **43** 1781–4
——1982 *Phys. Lett.* **114B** 111–14
Siemssen R H *et al* 1967 *Phys. Rev. Lett.* **19** 369–72

Sperr D *et al* 1976a *Phys. Rev. Lett.* **36** 405–8
——1976b *Phys. Rev. Lett.* **37** 321–3
Spinka H and Winkler H 1972 *Astrophys. J.* **174** 455–61
——1974 *Nucl. Phys.* A **233** 456–94
Stokstad R *et al* 1972 *Phys. Rev. Lett.* **28** 1523–5
Strasbourg 1994 *Proc. 6th Int. Conf. on Clusters in Nuclear Structure and Dynamics (Strasbourg, France)* unpublished
Sugiyama Y *et al* 1985 *Phys. Lett.* **159B** 90–4
Takigawa N and Arima A 1971 *Nucl. Phys.* A **168** 593–624
Trombik W *et al* 1984 *Phys. Lett.* **135B** 271–4
Turku 1992 *Proc. Int. Conf. on Clustering Phenomena in Atoms and Nuclei (Turku, Finland, 1991)* ed M Brenner, T Lönnroth and F B Malik (Heidelberg: Springer)
Vogt E W and McManus H 1960 *Phys. Rev. Lett.* **4** 518–20
Voit H *et al* 1977 *Phys. Lett.* **67B** 399–401
Wieland R M *et al* 1976 *Phys. Rev. Lett.* **37** 1458–61
Wilczynski J *et al* 1986 *Phys. Lett.* **181B** 229–32
Wuosmaa A H *et al* 1987a *Phys. Rev. Lett.* **58** 1312–5
——1987b *Phys. Rev.* C **36** 1011–5
——1990 *Phys. Rev.* C **41** 2666–80
——1992 *Phys. Rev. Lett.* **68** 1295–9
——1994a *Nucl. Instrum. Methods* A **345** 482–91
——1994b *Phys. Rev.* C **50** 2909–16
——1995 *Ann. Rev. Nucl. Part. Sci.* **45** 89–131
——1996 *Phys. Rev.* C **54** 2463–8
Zurmühle *et al* 1983 *Phys. Lett.* **129B** 384–6